[*]Research supported in part by the U. S. Air Force through Grant No. AF-AFOSR-1310-67.

[1]The abbreviations nn for nearest neighbor and nnn for next nearest neighbor are used throughout.

[2]V. G. Vaks, A. I. Larkin, and Yu. N. Ovchinnikov, Zh. Eksperim. i Teor. Fiz. $\underline{49}$, 1180 (1965) [Soviet Phys. JETP $\underline{22}$, 820 (1966)]. The union-jack lattice is just the dual of the bathroom-tile lattice.

[3]J. Stephenson and D. D. Betts, Phys. Rev. (to be published).

[4]The notation of "stability" is made quantitative for the triangular lattice by J. Stephenson, Can. J. Phys. $\underline{47}$, 2621 (1969).

[5]A detailed account of axial pair correlations on the triangular lattice is given by J. Stephenson, J. Math. Phys. $\underline{11}$, 413 (1970); $\underline{11}$, 420 (1970).

[6]H. A. Kramers and G. H. Wannier, Phys. Rev. $\underline{60}$, 252 (1941).

[7]J. S. Marsh, Phys. Rev. $\underline{145}$, 251 (1966).

[8]J. F. Dobson, J. Math. Phys. $\underline{10}$, 40 (1969).

[9]I. Syozi, Progr. Theoret. Phys. (Kyoto) $\underline{39}$, 1367 (1968).

[10]J. Stephenson, Can. J. Phys. (to be published).

[11]M. A. Moore, D. Jasnow, and M. Wortis, Phys. Rev. Letters $\underline{22}$, 940 (1969).

[12]M. E. Fisher, Rept. Progr. Phys. $\underline{30}$, 615 (1967).

[13]L. P. Kadanoff et al., Rev. Mod. Phys. $\underline{39}$, 395 (1967).

[14]M. E. Fisher and B. Widom, J. Chem. Phys. $\underline{50}$, 3756 (1969).

[15]C. Domb, Advan. Phys. $\underline{9}$, 149 (1960).

Phase Transitions and Soft Librational Modes in Cubic Crystals[*][†]

G. P. O'Leary[‡] and R. G. Wheeler

Mason Laboratory, Yale University, New Haven, Connecticut 06520

(Received 1 December 1969)

Landau's theory of second-order phase transitions and the theory of lattice dynamics are combined in a presentation of an approach to the understanding of the crystallographic phase transitions of complex fcc crystals. The approach is applied to the antifluorite-type crystal K_2ReCl_6, which exhibits four phase transitions. The results of a series of crystallographic and spectrographic experiments are described, and are interpreted in light of the developed theory. Finally, a model based on the theory is constructed and is shown to describe the spectral observations. The resultant model leads to the conclusion that two of the phase transitions are driven by a single branch of a "soft" phonon.

INTRODUCTION

This paper attempts to provide a single consistent theoretical picture for the understanding of all the experimental results related to the lattice dynamics and crystallographic phase transitions of crystals possessing the antifluorite (R_2MX_6) structure. This theoretical picture centers around the establishment that these materials exhibit phase transitions that are driven by a new type of soft mode. In fact, most of the observed transitions can be described in terms of the temperature dependence of a single branch of the phonon spectrum, the longitudinal rotary mode which involves librational motion of the $MX_6^=$ octahedron as a solid body. This mode is unique in the respect that it is a *gerade* phonon unlike the *ungerade* transverse optic mode that is responsible for the $BaTiO_3$ ferroelectric transition.[1-5] The system R_2MX_6 is singular in that a single branch of the spectrum can describe transitions involving no change in the number of molecules per unit cell and also transitions involving doubling or quadrupling of the number of molecules per cell.

In developing a model for this system, we were spurred on by the belief that it is possible to obtain a rather detailed understanding of the lattice dynamics and phonon spectrum of a relatively complicated structure via imaginative use of traditional and readily available experimental techniques. In order to glean the maximum amount of information from these techniques, however, it is necessary to utilize a combined theoretical and experimental approach. We will be attempting to show here that a description of such a system is possible when a theoretical calculation is carried out in close connection with experiment. Thus, theoretical and experimental results will be interspersed in an attempt to demonstrate the close relationship between the two that is all important in such an undertaking.

The particular antifluorite structure that we are concerned with here is essentially the same as CaF_2, except for the replacement of the F^- by a positive ion R^+, and the Ca^{++} by the octahedral anion $MX_6^=$, indicated in Fig. 1. The extra degrees
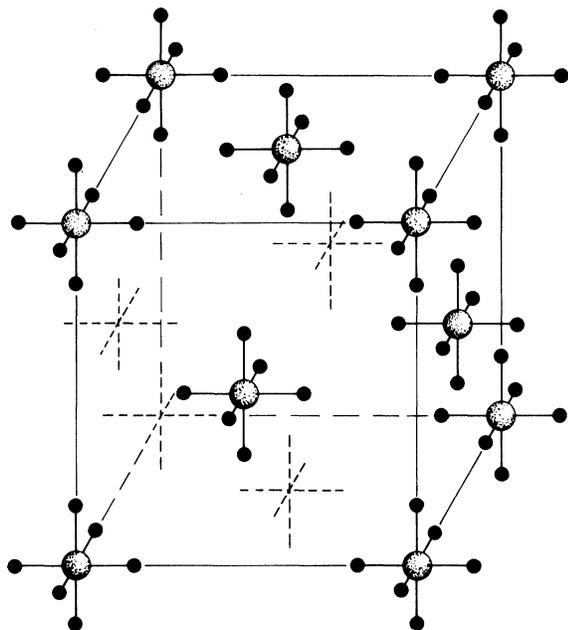
FIG. 1. Relative positions and orientations of the MX_6 octahedra in the face-centered lattice. Not shown are the positive-ion positions R^+ which are arranged to fill the simple cubic interstices about the MX_6 octahedra.

of freedom supplied by the anion give rise to the complications and also to the interesting features of this structure. The major difficulty with this type of crystal lies in the fact that the M-X distance is not determined by symmetry. This is in contrast to all the other structures for which calculations of the elementary excitations, the phonons, have been attempted. The major interesting feature, on the other hand, is the observed crystallographic phase transitions of this class of crystals.

The thrust of the theoretical work to be presented is twofold. The major effort lies in the rigid-ion lattice-dynamics calculation of the dispersion relations of the phonon spectrum while the secondary and yet totally interrelated effort is involved in the establishment of symmetry-based relationships between the structures which occur in the various phase transitions. The experimental work, on the other hand, has culminated in an intensive study of a particularly interesting example of this series of salts, namely, K_2ReCl_6. In addition to a transition to an antiferromagnetically ordered state at 12 °K, it undergoes three crystallographic changes between 76 and 110.9 °K.[6] The specific-heat curves of Busey, Dearman, and Bevan illustrating the first evidence for these

transitions are depicted in Fig. 2. We will be describing here experiments which give new information about the thermodynamic order of the transitions and also about the nature of the atomic displacements involved in each. We will also be describing a series of spectroscopic experiments which supply enough information for an unambiguous least-squares fit in the lattice-dynamics calculation. With this particular example in hand, it then turns out to be possible to apply the ideas developed here to describe the behavior of a surprisingly large class of materials.

Historically, this work began with an attempted study of the antiferromagnetic phase of K_2ReCl_6. The hope was that one could observe the elementary excitations of the magnetic system, the spin waves, as far-infrared absorptions. Fortunately or unfortunately, as the case may be, several new absorptions appeared in the magnetic phase but at the time none of them could be shown to be magnons. In particular, the strongest, sharpest, new features of the spectrum and hence the first ones to be observed were insensitive to magnetic fields as high as 140 kG. A theoretical spin-wave calculation based on the magnetic symmetry[7] determined from elastic neutron-diffraction experi-
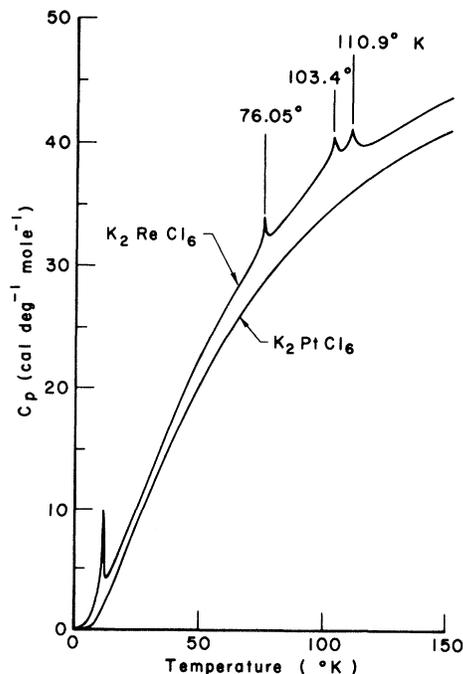
FIG. 2. Heat-capacity data on K_2ReCl_6 of Busey, Dearman, and Bevan[6] are shown compared with the isomorphic salt K_2PtCl_6 which does not undergo any phase transitions.

ments demonstrated that such insensitive excitations could not be spin waves. It was clear that a knowledge of the magnetic symmetry alone was not sufficient for the understanding of the infrared spectra.

A series of nonmagnetic experiments was embarked upon. The first of these was an attempt to elucidate the relation between the far-infrared spectrum and the crystallographic symmetry via temperature-dependent infrared studies. This led finally to x-ray determinations of the crystal structure over most of the temperature range. The present work results from the fact that the relations between the spectra and the crystallographic phase transitions rapidly became as interesting and as theoretically promising as the spin waves and magnetic transition had once seemed.

A word should be added here at the start about the spirit in which this investigation was carried out. It has been observed that the static parameters (long-range order, specific heat, etc.) of many different kinds of phase transition behave qualitatively (and in some cases quantitatively) in similar fashion.[8,9] A twofold suspicion is aroused by this behavior. On the one hand, one would like to say that perhaps such similar behavior is fundamental. This approach leads to ideas such as the scaling laws and also to attempts by experimentalists to force disparate phase transitions to fit one or two hypothetical models. On the other hand, the concern arises that perhaps such static quantities are not very sensitive to the details of the particular phase transition involved. This alternative leads one to look for theories and experiments that will elicit the true microscopic dynamic behavior. An attempt has been made to utilize both approaches here. The experiments have been analyzed for both their static and dynamic content. The prejudice, however, is in that direction which leads to a dynamic model of the phase transitions under consideration.

The model to which we have been led implies that the octahedral (MX_6) anion behaves as a rigid body at these phase transitions. The discussion will focus upon the stability of the lattice mode which describes the rotational oscillation of the rigid anion within the cation (R_2) environment. The theory will indicate how the symmetry and energy of the mode are connected with the phase transitions, and will allow predictions of the spectroscopically observable phonon states. New experimental results on K_2ReCl_6 will illustrate the applicability of the theory to the interrelated problems of determining crystal symmetry and identifying phonon states. The data will allow the lattice-dynamics calculation which shows that this rotary mode may be "soft" in the sense discussed

by Anderson, Cochran, and Cowley.[1-3] Direct observation of this soft mode has been made in the low-temperature phases. Finally, nuclear-quadrupole-resonance data are presented which indicate that the chlorine displacements are consistent with the soft-mode hypothesis at temperatures both above and below the phase transitions. These last results will be shown to be inconsistent with the alternative explanation in terms of an order-disorder phase transition and thus provide perhaps the most clinching argument in favor of the soft-mode description.

THEORY

The major problem that presents itself here is the elucidation of a theoretical model that will adequately describe the lattice dynamics and the observed crystallographic transitions of the antifluorite R_2MX_6 class of salts. As has been intimated in the Introduction, the presence of a soft mode forces one to construct a theory that interrelates lattice dynamics and phase transitions. Landau's theory of second-order phase transitions will be described for the sake of its group-theoretic content, which makes possible predictions of the symmetries that can be obtained in crystallographic phase transitions. Lattice dynamics in the rigid-ion model will be discussed in enough detail to prepare the way for calculations on K_2ReCl_6. The presentation of these two theories side by side will allow us to state more clearly than has been done in the past the connection between the theory of Landau[10] and the soft-mode approach to phase transitions. In order to provide a common denominator of notation, we will begin with the lattice-dynamics discussion.

The underlying feature of our approach is the assumption that one can calculate to a fair degree of precision the properties of the distorted phases on the basis of the undistorted fcc phase. There exists good experimental evidence for this approach, since crystal structure and optical measurements indicate that the internal displacements involved in the distortions of these salts are very small. More important, however, is the fact that most of the vibrational spectrum, with one very important exception, is insensitive energetically to the phase transitions. Thus, a classification of vibrational modes based on their symmetry properties in the fcc phase provides a convenient and conceptually simple means of keeping track of them as a function of temperature. In addition, the observed insensitivity implies that a lattice-dynamics calculation based on the high-symmetry structure should be able to provide us with a reasonable fit to all but the soft mode itself.

Traditionally, attempts at classifying vibrational

spectra commence with a factor-group analysis of the basis functions for normal modes of infinite wavelength.[11] This procedure will be insufficient here since, as we shall see later, the lattice distortions will make possible the direct observation of phonons of nonzero fcc wave vector. Note that it is just these observations that will provide the extra information necessary for the lattice-dynamics calculation. Thus, one needs to construct a generalized factor-group analysis that can handle normal modes of arbitrary wavelength. Such group-theoretical considerations are useful in two ways. They often allow one to assign labels to spectral features on the basis of symmetry alone, and they provide a qualitative check on any numerical calculations that may follow.

Given a crystal composed of N molecules with n atoms per molecule, the basis functions for all the normal modes of the crystal must be linear combinations of the $3Nn$ possible independent translations of all the atoms making up the crystal. These $3Nn$ displacements, $u_x(l, n)$, $u_y(l, n)$, $u_z(l, n)$, of the nth atom in the lth cell form a basis for a reducible representation of the full space group describing the translational and rotational symmetry of the crystal. The projection of this reducible representation[12] along the various irreducible representations of the space group will generate the basis functions of the normal modes transforming according to each. Such a procedure, of course, would be rather impractical in the most general case. However, for normal modes whose wavelengths are commensurate with a small number of lattice constants, it is possible to construct their basis functions by considering a miniature crystal or supercell of side equal to the wavelength of the normal mode whose basis function is desired. The reducible representation thus generated will contain the basis functions for phonons of the wavelength of interest and also for all other wavelengths commensurate with the length of the side of the supercell. Thus, the basis functions will always include those of infinite wavelength since a wave of length equal to the side of the true primitive cell which contains only one molecule is equivalent to a wave of infinite length.

The remaining factor that is needed to carry out the projection is a knowledge of the characters of the irreducible representations of the full space group. The procedure for generating these characters is well known and has been adequately described elsewhere.[12-15] In fact, complete tabulations now exist for O_h^5 and for all the space groups and magnetic space groups.[16-18]

The reduction of the basis functions for lattice vibrations of wave vector Γ and X is given in Table I. In addition to a simple labeling according to ir-

reducible representation the basis functions are given as complete a physical description as is possible from symmetry alone. It is this physical description that will allow us to begin to sort out the experimental observations. Note that the fcc labels given to the basis functions here will be used throughout the discussion including that of the phonons in the distorted phases.

The wavelengths of electromagnetic radiation used in far-infrared and Raman spectroscopy are several orders of magnitude larger than the lattice constant. Conservation of momentum $p = h/\lambda$ thus requires that the wave vector of any phonon created or destroyed by such radiation be very close to $\vec{k}$ $= 0$. In the fcc phase, then, one should be able to classify all observed excitations approximately according to the Γ point listing given in Table I.

TABLE I. Group-theoretical basis functions.

Irreducible representation	No. of modes	Activity	Description
$\Gamma^{1+}(\nu_1)$	1	Raman	ν_1 internal breathing mode
$\Gamma^{3+}(\nu_2)$	1	Raman	ν_2 internal
Γ^{4+}	1[a]	Silent	Rotary mode
$\Gamma^{5+}(\nu_5)$	1	Raman	ν_5 internal
Γ^{5+}	1	Raman	K^+ motion
Γ^{4-}	1	$\cdots$	Acoustic
$\Gamma^{4-}(\nu_3 \& \nu_4)$	2	Infrared	$\nu_3 \& \nu_4$ internal
Γ^{4-}	1	Infrared	Optic mode
$\Gamma^{5-}(\nu_6)$	1[a]	Silent	ν_6 internal
X^{1+}	3	$\cdots$	ν_1 at X, one branch of ν_2, and longitudinal K^+ motion
X^{2+}	1[b]	Raman	Second branch of ν_2
X^{3+}	1[b]	Raman	Longitudinal ν_5
X^{4+}	1[b]	Raman	Longitudinal rotary mode
X^{5+}	3[b]	Raman	Transverse: K^+ motion, rotary mode, and ν_5
X^{2-}	1		Longitudinal K^+ motion
X^{3-}	1		Longitudinal ν_6
X^{4-}	3		Longitudinal: acoustic, ν_3, and ν_4
X^{5-}	5[b]	Infrared	Transverse: acoustic, K^+ motion, ν_3, ν_4, and ν_6

[a]Modes which become first-order active due to Γ^{4+} distortion.

[b]Modes which become first-order active due to X^{4+} distortion. X-point activity indicated is that due to X^{4+} distortion.

Clearly, the existence of three infrared-active and two Γ^{5+} Raman-active species implies that one will have to apply some physical arguments to the assignment of basis functions to the fcc spectra. An important observation must be made here about the role that is played by the translation symmetry of the lattice. It is the translation symmetry that is all important in partially removing this restriction to $\vec{k} = 0$ and thus in allowing conventional techniques to obtain information about the dispersion relations of the phonons.

The space group of K_2ReCl_6 at room temperature[19] is fcc or O_h^5 in the Schöenflies notation. Its primitive translation vectors are given by

$$\vec{t}_1 = (\tfrac{1}{2}, \tfrac{1}{2}, 0)a, \quad \vec{t}_2 = (\tfrac{1}{2}, 0, \tfrac{1}{2})a, \quad \text{and} \quad \vec{t}_3 = (0, \tfrac{1}{2}, \tfrac{1}{2})a \quad , \quad (1)$$

where $a = 9.84$ Å is the side of the simple cubic cell. The reciprocal-lattice vectors conjugate to the above are

$$\vec{b}_1 = (1, 1, -1)/a, \quad \vec{b}_2 = (1, -1, 1)/a, \quad \vec{b}_3 = (-1, 1, 1)/a. \quad (2)$$

These are just the primitive vectors of a bcc lattice. The Brillouin zone corresponding to these vectors is shown in Fig. 3. Of particular interest are the high-symmetry points labeled Γ, X, and L with wave vectors $(0, 0, 0)$, $(1/a, 0, 0)$, and $(\tfrac{1}{2}, \tfrac{1}{2}, \tfrac{1}{2})/a$, respectively.

A primary concern in what follows will be the relationship of this zone to those of the structures that will obtain in the low-temperature distorted phases. For example, consider the case of the symmetry T_h^2 determined at 20 °K by elastic neutron-diffraction measurements on K_2ReCl_6.[7] In this structure the primitive translation vectors

FIG. 3. fcc Brillouin zone is shown with the high-symmetry points Γ, X, L designated. Inscribed within is the zone for the T_h^2 four molecule/unit cell structure. Note that the L point remains common to both zones.

are given by

$$\vec{t}_1 = (a, 0, 0), \quad \vec{t}_2 = (0, a, 0), \quad \text{and} \quad \vec{t}_3 = (0, 0, a) \quad . \quad (3)$$

There are four molecules per primitive cell in this structure, and thus the volume of the unit cell is four times that of the fcc cell. The T_h^2 reciprocal-lattice vectors then are given by

$$\vec{b}_1 = (1/a, 0, 0), \quad \vec{b}_2 = (0, 1/a, 0), \quad \text{and} \quad \vec{b}_3 = (0, 0, 1/a). \quad (4)$$

One can see immediately that the $\vec{X}_x$ point equals $(1/a, 0, 0)$ of the fcc zone is identical with the reciprocal-lattice vector $\vec{b}_1$ of the T_h^2 reciprocal lattice. Thus, a wave of wave vector equal to X in the fcc phase must become a wave of wave vector equal to zero in the distorted phase. Perhaps a physical picture would be useful. In O_h^5 there is one K_2ReCl_6 molecule per primitive unit cell; thus, a lattice vibration of wavelength equal to X corresponds to a situation in which neighboring unit cells are moving out of phase. In T_h^2, however, there are four molecules per unit cell, and a vibration of this same wavelength corresponds to an internal motion of the unit cell with all the unit cells of the crystal moving in phase. Hence, it has become a wave of infinite wavelength.

The appearance of new phonons of infinite wavelength then may be an indication of a distortion involving a change in the number of molecules per unit cell. Conversely, a knowledge of the number of molecules per unit cell in a structure resulting from a distortion may allow the identification of the fcc wave vectors of the new phonons observed in the lower-symmetry phase. Thus, a small displacement distortion may allow the determination of the amount of dispersion present in the various branches of the phonon spectrum.

With the group-theoretical description of the modes in hand, let us turn to the necessary mechanics of the actual lattice-dynamics calculation. The notation will be presented in detail in an attempt to pave the way for the application of Landau's phase-transition theory and to make the ensuing calculations clear. The R_2MX_6 fcc structure is slightly more complicated than the other structures for which complete lattice-dynamic calculations have been performed. The complication lies in the fact that the M-X separation is a free parameter not determined by the crystallographic symmetry. Thus, the dynamic force constants used in the calculation must be consistent with the observed static separation of the atoms. In addition, the simplifications that arise when all of the atoms sit at centers of symmetry will not be present for this structure. These difficulties could in
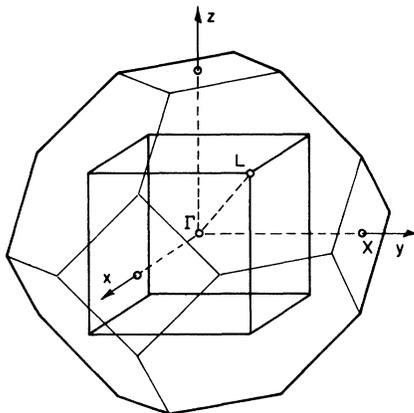
principle be eliminated by considering an imagi-
nary structure in which the $MX_6^=$ octahedra are sol-
id bodies. Unfortunately, the algebraic problems
associated with an extended-body octahedron are
almost as severe as the bookkeeping troubles that
arise from considering all the atoms as indepen-
dent. Thus, we will proceed in an essentially
brute-force manner, considering the interactions
between as large a number of atoms as possible.
The calculation, of course, will be based on the
assumption of fcc symmetry. As has been argued
above, the energies thus determined should be
nearly identical to those found in the distorted
phases with the exception perhaps of the soft-rotary
mode.

We must also recognize that the amount of in-
formation about the frequencies of the phonons will
be limited, since we will know the energies at only
a few high-symmetry points of the Brillouin zone.
Thus, we need a model possessing a minimum
number of free parameters. The model to be used
assumes that the ions are rigid (nonpolarizable) in-
teracting with central forces that can be separated
into a short-range part that acts between near
neighbor atoms only and a long-range electrostatic
interaction due to the ionic charges. The prime
limitation of such a model is that it cannot give an
adequate description of the high-frequency dielec-
tric constant of the crystal since it does not include
the polarizabilities of the ions. A major reason
for hope, however, lies in the fact that this model
provides an extremely good description of the pho-
non spectrum of CaF_2 and UO_2.[20,21] In fact, if one
ignores the high-frequency dielectric-constant
failing of the rigid-ion model, the agreement be-
tween theory and experiment in UO_2 improves by
only a few percent when one goes to the more com-
plicated shell models.[21]

The general theory of lattice dynamics due to
Born and Huang[22] begins in the adiabatic approxi-
mation with the assumption of the existence of a
function U which expresses the potential energy of
the whole crystal in terms of the positions of all
the atoms in it. This potential is expanded in terms
of small displacements $\vec{u}(l, n)$ of the nth atom in the
lth unit cell from its equilibrium position $\vec{X}(l, n)$.
The harmonic approximation involves the ignoring
of all derivatives higher than the second. The
Hamiltonian for this system is

$$H = \sum_{n,l,\alpha} \frac{1}{2M_n} p_\alpha^2(l, n)$$
$$+ \frac{1}{2} \sum_{n,l,\alpha;n',l',\beta} U_{\alpha\beta}(l, n; l'n')u_\alpha(l, n)u_\beta(l', n') ,$$

(5)

where M_n and $p_\alpha(l, n)$ are, respectively, the mass

and the momentum operator of the (l, n)th atom,
and the $U_{\alpha\beta}(l, n; l', n')$ are the second derivatives
of the potential energy with respect to the coordi-
nates of the (l, n) and the $(l' n')$ atoms. The nota-
tion used is essentially the same as that of Born
and Huang.

This Hamiltonian describes a system of coupled
simple harmonic oscillators. Thus, the energies
of the normal modes must be given by the solution
of the equivalent classical problem which is com-
prised of the $3nN$ Lagrange equations,

$$M_n\ddot{u}_\alpha(l, n) = - \sum_{n',l',\beta} U_{\alpha\beta}(l, n; l', n')u_\beta(l', n') .$$
(6)

Any attempt to decouple these equations would be
foolhardy unless one made use of the translation
symmetry of the lattice. A physical solution of a
set of equations of motion for a periodic structure
must be expressible in terms of running waves of
wave vector $\vec{k}$ where $\vec{k}$ lies within the first Bril-
louin zone of the structure. In addition, we can
see that the solutions must have a simple harmonic,
sinusoidal time dependence. Thus, for the solution
one tries a linear transformation of the displace-
ments,

$$u_\alpha(l, n) = \frac{1}{(NM_n)^{1/2}} \sum_{\vec{k},j} e_\alpha(n|\vec{k}, j)Q(\vec{k}, j)$$
$$\times \exp[2\pi i\vec{k} \cdot \vec{X}(l) - i\omega(\vec{k}, j)t] ,$$
(7)

where N is the number of unit cells in the crystal
and $\vec{X}(l)$ is a vector specifying the position of the
origin of the lth primitive cell in the lattice. Sub-
stitution of this expression into the equations of
motion yields the following which must be satisfied
by the eigenvectors $e_\alpha(n|\vec{k}, j)$ and eigenvalues
$\omega(\vec{k}, j)$ in order for there to be a solution:

$$\sum_{n',\beta} D_{\alpha\beta}(\vec{k}; n, n')e_\beta(n'|\vec{k}, j) = \omega^2(\vec{k}, j)e_\alpha(n|\vec{k}, j) ,$$ (8)

where $D_{\alpha\beta}(\vec{k}; n, n')$ is the Fourier transform of the
second derivatives of the potential.

$$D_{\alpha\beta}(\vec{k}; n, n') = \sum_l \frac{1}{(M_nM_{n'})^{1/2}}$$
$$\times U_{\alpha\beta}(0, n; l, n')\exp[-2\pi i\vec{k} \cdot X(l)] .$$ (9)

Thus, the eigenvectors and eigenvalues result
from the diagonalization of the dynamic matrix
$D_{\alpha\beta}(\vec{k}; n, n')$ for each value of $\vec{k}$. The indices of
the dynamic matrix are the coordinate labels α, β
= 1, 2, 3 and the atom labels n, n' which run over
all the atoms in the unit cell. For R_2MX_6 with
nine atoms per primitive cell, it is a 27×27 ma-
trix. In general, there result 27 energies for
every value of $\vec{k}$. These 27 energies would each
be specified by the branch label j. For the sake
of simplifying the notation, we will follow Cow-

ley's[3] convention of representing the quantum numbers $(\vec{k}, j)$ by the single quantum number λ, where $-\lambda$ is understood to mean $(-\vec{k}, j)$. Note that these quantum numbers are exactly equivalent to the group-theoretical labels introduced above. They are slightly more specific in that the branch j details not only the particular representation of the group of the wave vector, but also the actual basis function (in the case of degenerate vibrations) corresponding to the λth phonon.

If one applies the above linear transformation Eq. (7) to the operators appearing in the Hamiltonian, one obtains

$$H^0 = \tfrac{1}{2} \sum_\lambda [\dot{Q}^*(\lambda)\dot{Q}(\lambda) + \omega^2(\lambda)Q^*(\lambda)Q(\lambda)] \ . \quad (10)$$

The Hamiltonian has been transformed into one describing a collection of uncoupled simple harmonic oscillators specified by operators $Q(\lambda)$, known as the complex-normal coordinates. Physically these operators correspond to the amplitude of the atomic displacements in the λth normal mode, while the eigenvectors $e_\alpha(n|\lambda)$ specify the relative displacements of the nth atom in the unit cell in the αth direction.

The complex-normal coordinates are related in the usual way to the creation and destruction operators for the phonons,

$$Q(\lambda) = [\hbar/2\omega(\lambda)]^{1/2}[a(\lambda) + a^*(\lambda)] \ , \quad (11)$$

$$\dot{Q}(\lambda) = i[\tfrac{1}{2}\hbar\omega(\lambda)]^{1/2}[a^*(\lambda) - a(\lambda)] \ . \quad (12)$$

Thus, the expectation values of the real coordinates can be determined in terms of those of the operators, for example,

$$\langle u_\alpha^2(l, n)\rangle = \frac{\hbar}{NM_n} \sum_\lambda |e_\alpha(n|\lambda)|^2 \frac{[n(\lambda) + \tfrac{1}{2}]}{\omega(\lambda)} \ , \quad (13)$$

where $n(\lambda)$ is the Bose population factor for the λth normal mode. The results of the diagonalization of the dynamic matrix thus can be used quite easily to generate quantities such as the average rotation angle of the octahedra that will come into the discussion of the nuclear-quadrupole resonance. In addition, we see here once again the relation between the eigenvectors and the actual displacements of the atoms.

The energies and eigenfunctions as determined by the type of harmonic approximation given above will be strictly independent of temperature unless one inserts an *ad hoc* temperature dependence into the second derivatives of the potential-energy function. This approach to the problem of introducing temperature-dependent phonon frequencies is the simplest version of the quasiharmonic approximation. Essentially, it amounts to a static inclusion of the effects of lattice expansion on the inter-

atomic force constants. As Cowley has pointed out, however, this type of approximation is inadequate in situations where the phonon energies approach zero.[3] In such cases one should proceed by explicitly including the anharmonic effects responsible for the temperature dependence of the phonon frequencies. This is done via a many-body calculation which includes the higher derivatives of the potential-energy function. We will not attempt in this paper to carry out a complete many-body-type calculation of the renormalized energies. We will, however, describe this approach in sufficient detail to allow us to bring to bear once again the powerful tools of group theory.

The complex-normal coordinates of the simple harmonic Hamiltonian are very useful for organizing and discussing the higher derivatives of the potential-energy function. Simple substitution of the above linear transformation of the real displacements into the expressions for the higher derivatives in the Hamiltonian yields for the third-order term, for example,

$$H^{(3)} = \frac{1}{6(N)^{1/2}} \sum_{\lambda, \lambda', \lambda''} \Delta(\vec{k} + \vec{k}' + \vec{k}'')$$
$$\times V(\lambda, \lambda', \lambda'')Q(\lambda)Q(\lambda')Q(\lambda'') \ , \quad (14)$$

where the Δ function as usual implies that the sum of wave vectors must equal a reciprocal-lattice vector, and the anharmonic coefficient is given by

$$V(\lambda, \lambda', \lambda'') = \sum_{l', l''; n, n', n''; \alpha, \beta, \gamma} \frac{1}{(M_n M_n' M_n'')^{1/2}}$$
$$\times U_{\alpha\beta\gamma}(0, n; l', n'; l'', n'')e_\alpha(n|\lambda)e_\beta(n'|\lambda')$$
$$\times e_\gamma(n''|\lambda'') \exp\{2\pi i[\vec{k}' \cdot \vec{X}(l') + \vec{k}'' \cdot \vec{X}(l'')]\} \ . \quad (15)$$

Forbidding as this expression may appear, it is just the projection of the derivatives of the potential along the normal modes. The form of Eq. (14) and of the other similar expressions that result for all the higher-order terms in the expansion of the Hamiltonian is such as to allow a simple group-theoretical discussion of their properties.

In diverting our attention from the real displacements of the atoms in the crystal to the complex-normal coordinates, we have also transferred all the transformation properties of the displacements onto the $Q(\lambda)$ in such a way that they form a basis for the λth irreducible representation of the space group. They must form such a basis because they are the operators that diagonalize the simple harmonic Hamiltonian. If the higher-order terms in the Hamiltonian are to provide a physical description of the dynamics of the crystal, then they must be totally symmetric under all the symmetry operations. It must be an invariant. Thus, for ex-

ample, the only allowed third-order coefficients $V(\lambda, \lambda', \lambda'')$ are those which produce invariant linear combinations of triple products of the complex-normal coordinates Q.

These invariant triple products are just those for which the product of the three representations, according to which the phonons λ, λ', and λ'' transform, contains the identity representation. Such group-theoretical products have been worked out for all the symmetry points of the fcc Brillouin zone by Chen, Berenson, and Birman.[23] For the cases of interest we will be able to use their tabulation of products to determine the allowed terms in the Hamiltonian. Cowley, of course, goes on to show how the temperature-dependent frequencies of the normal modes may be calculated in terms of the anharmonic coefficients and the harmonic frequencies. His explicit results will not be needed, however, for the discussion at hand.

Perhaps the most useful feature of the anharmonic terms in the Hamiltonian is their ability to describe the properties of a slightly distorted phase. The harmonic phonon eigenfunctions provide a complete set of states for describing small displacements of the atoms from their high-symmetry equilibrium positions. Thus, in a crystallographic phase change involving small motions of the atoms, the static atomic displacements must be expressible as a linear combination of the phonon eigenvectors. In particular, if the distortion can be described in terms of a single phonon basis function, then

$$u_\alpha(l, n) = (NM_n)^{-1/2} e_\alpha(n|\lambda)\langle Q(\lambda)\rangle$$
$$\times \exp[2\pi i \vec{k} \cdot \vec{X}(l)] \qquad (16)$$

will be the static displacement of the (l, n)th atom and the expectation value $\langle Q(\lambda)\rangle/N^{1/2}$ will serve as an order parameter $\eta(\lambda)$ of the phase transition. Replacement of one of the operators in the third-order Hamiltonian with this static expectation value has the effect of adding new terms into the simple-harmonic part which becomes

$$H^0 = \tfrac{1}{2}\sum_{\lambda'} \left(\dot{Q}^*(\lambda')\dot{Q}(\lambda') + \omega_0^2(\lambda')Q^*(\lambda')Q(\lambda')\right.$$
$$\left. + \sum_{\lambda''} \Delta(\vec{k}+\vec{k}'+\vec{k}'')V(\lambda\lambda'\lambda'')\eta(\lambda)Q(\lambda')Q(\lambda'')\right).$$
$$(17)$$

This again is just a system of coupled simple-harmonic oscillators which can be solved by a brute-force rediagonalization or by an application of first-order perturbation theory. The solutions will give the new normal coordinates as linear combinations of the old, or, which is the equivalent, will give the new eigenvectors of the normal modes. Higher-order derivatives will enter into this new harmonic Hamiltonian with higher powers of the

order parameter and thus may be neglected as far as the renormalization of the basis functions is concerned.

This distorted-phase Hamiltonian is very useful for discussing the active vibrational excitations of that phase. A particular phonon (λ') will become active if there is a term in this Hamiltonian coupling it with one of the fcc Γ-point active phonons. Thus, the (λ'') phonon in the above expression will have to be a Γ-point normal mode. The phonon (λ) is, of course, the one characterizing the distortion. The wave-vector δ function then tells us immediately that $\vec{k}+\vec{k}'$ must equal a reciprocal-lattice vector. Thus, if the distortion is characterized by a Γ-point phonon, $\vec{k}=0$, then $\vec{k}'$ must also equal zero. The only phonons whose activity is affected by a transition involving no change in the number of molecules per cell are those of infinite wavelength in the fcc structure. But if the distortion is characterized by a phonon of wave vector equal to $\vec{X}$, then those phonons having the same wave vector as the distortion will become active. Remember that the above expression for the Hamiltonian is written only to first order in the distortion; thus its predictions for activity will not coincide completely with complete group-theoretical predictions based on the crystallographic symmetry. This fact is extremely useful, however. The first-order Hamiltonian will predict which will be the most strongly active phonons in the distorted phase and thus will help tremendously with the assignment of basis functions to the features of the spectra.

Looking ahead a bit to our discussion of the transitions of the R_2MX_6 salts, we have applied this Hamiltonian, Eq. (17), to distortions which look like the Γ^{4+} and the X^{4+} phonon eigenvectors. To answer the question as to which phonons will become active, one simply has to use the tables of products of fcc representations[23] to determine the allowed third-order invariants that can be constructed from the Γ^{4+} or X^{4+} distortion phonons and the Γ-point infrared and Raman active phonons. The results of this analysis are indicated in Table I. The most interesting feature of these results is the fact that the number of phonons that become active to the order of this Hamiltonian is considerably smaller than the number that we will show to be active on the basis of the symmetry produced by these two types of distortion.

There is one feature of Cowley's explicit results that will be extremely useful for our discussion. In addition to calculating expressions for the temperature-dependent phonon frequencies, he goes on to write the Helmholtz free energy of a distorted crystal. The lowest-order contribution is given by

$$\Delta F = \omega_T(\lambda)^2 \eta(\lambda)^2 \quad , \tag{18}$$

where $\eta(\lambda)$ is the order parameter of the distortion as described above and $\omega_T(\lambda)$ is the temperature-dependent frequency of the λth mode when $\omega_T(\lambda)$ is near zero. The higher-order terms in this expansion of the free energy in the distortion turn out to be proportional to the higher-order terms in the Taylor's series expansion of the Hamiltonian. The amazing thing is that the Hamiltonian of the undistorted phase can be used to describe the properties of the lower-symmetry phase. We will discuss in a moment the actual conditions that must be met for such expansions to be valid. Note, however, that the requirement of a small-displacement distortion is of prime importance.

The basic theory of displacive transitions is originally due to Landau.[10] It is a static thermodynamic theory in that it assumes the existence of a Gibbs free energy which is a minimum at all temperatures including the transition temperature itself. For historical reasons, it is referred to as Landau's theory of second-order phase transitions. This title is somewhat misleading, since it can be applied to phase transitions of first order provided the displacements involved are small.

A fundamental difficulty arises in the theory when it is applied to second-order phase transitions. The form assumed for the free energy is that of an expansion in the mean displacements involved in the transition. The difficulty presents itself when one realizes that near the transition temperature the thermally excited time-dependent fluctuations in the atomic positions may be larger than the mean displacements. Since the mean displacements must increase continuously from zero in order for a transition to be of second order, there will always be a temperature region in which the fluctuations will dominate. This region is called the critical region.

The theory is defended by the argument that for temperatures outside of the critical region, the free-energy expansion is valid. The crystal must take on the structure that minimizes this free energy. Thus the critical region remains as a "black box" from which the crystal emerges with the predicted symmetry, although one cannot say for certain what symmetry it may have had while in that region. Once again, the fact that the displacements are small plays an important role. Such small motions cannot significantly affect the form of the free-energy function even if they take place as fluctuations in the critical region.

Thus, one would like some estimate of the size of this critical-temperature region. Ginzburg[24] has been able to show that for the case of ferroelectric phase transitions the critical region oc-

curs for temperature deviations $(T_c - T)$ less than 10^{-3} of the transition temperature T_c. His discussion is based on the relatively long range of the electric dipole forces and the small magnitude of the volume energy associated with such transitions. There is reason to believe that such considerations should hold for the antifluorite transitions since there are long-range electrostatic forces acting, and once again, the small displacements imply that the change in free energy accompanying the transition will be small. An alternate approach is simply to use the anomalous region of the specific heat as an estimate of the critical region. Landau's theory predicts a simple discontinuity in the specific heat for a second-order phase transition. The temperature region of deviation from this simple behavior should thus give an estimate of the range in which the theory is invalid.

The great appeal of this theory is its simplicity. The detailed predictions that it makes for the behavior of such quantities as the long-range order and specific heat turn out to be not very well obeyed in practice, even in situations where they should be, such as the ferroelectrics. The more general group-theoretical predictions that it makes, however, do seem to conform to reality. Thus, it is mainly for this symmetry content that the theory will be presented and used here.

Our present aim then is to obtain an expansion of the free energy in terms of the small displacements of the atoms. The discussion given here will essentially parallel that of Landau and Lifshitz.[10] The results, however, will be presented in a slightly more general form, and the connection with the theory of lattice dynamics will be demonstrated. The Gibbs free energy is expanded in a Taylor's series in an order parameter

$$\Phi(P, T, \eta) = \Phi_0 + \alpha\eta + A(P, T)\eta^2$$

$$+ B(P, T)\eta^3 + C(P, T)\eta^4 + \text{etc.} \tag{19}$$

P and T are the pressure and temperature, respectively, and η, the order parameter, is a generalized coordinate describing the amplitude of the mean displacements of the atoms from their high-symmetry positions. Throughout this discussion, we will be concerned with transitions which occur at constant pressure, thus, the pressure dependence of the Gibbs free energy will be ignored. In addition, the transitions of interest will occur at constant volume, so that the Gibbs and Helmholtz free energies may be used interchangeably. Stability requires that the free energy be a minimum for all temperatures. Clearly then, $\alpha = 0$ identically. In the high-symmetry phase, the minimum must occur for $\eta = 0$, thus $A(P, T)$ must be greater than zero in that phase. This expansion now can

be used to discuss both first- and second- or even higher-order transitions.

In a second-order phase transition, the order parameter must change continuously starting from zero at the transition temperature T_c. In light of the above expansion, this is the equivalent of insisting that the free energy be continuous across the transition. For argument's sake let us assume that the high-symmetry phase is the high-temperature phase, although situations exist in which the reverse is the case. For η to change continuously at the transition temperature from a value of zero above to a finite value below, the following conditions must obtain:

$$A > 0 \quad \text{for} \quad T > T_c \ , \tag{20}$$

$$A < 0 \quad \text{for} \quad T < T_c \tag{21}$$

with $B = 0$ and $C > 0$ for temperatures immediately above and below T_c. The positive value of C is needed to assure that η remains finite at the transition, while the vanishing of B assures that the change will be continuous. Minimization of the free energy with respect to η for temperature above and below T_c leads to

$$\eta^2 = 0, \qquad T > T_c \tag{22}$$

$$\eta^2 = -A/2C, \quad T < T_c \ . \tag{23}$$

At this point, then, one is tempted to try to make an assumption about the behavior of A as a function of temperature near T_c. Since it passes through zero, the most obvious tack is to use the first term of a Taylor's series in the temperature difference. Thus, we have the classical prediction

$$A(T) = a(T - T_c) \ , \tag{24}$$

$$\eta^2 = a(T_c - T)/2C \ . \tag{25}$$

There is no fundamental basis for this assumption. In fact, from this discussion of fluctuations given above, we can see that it is a prediction made for the region in which the theory is least likely to work. It is interesting to note that other theories which make this assumption, i.e., that the first term in a perturbation series will dominate, also obtain this result.[1,3]

The only results that will be needed in what follows, however, are the relative signs of A and C and the fact that $B = 0$. These relative magnitudes are all that is necessary for a second-order transition. One can see that they do produce such a transition, since the discontinuity occurs in the second derivative of the free energy.

Similar arguments can be used to discuss a first-order transition in which η and $\partial\Phi/\partial T$ have a discontinuity at T_c. In this case the coefficient B

is nonvanishing, and one minimizes

$$\Phi(\eta) = A\eta^2 + B\eta^3 + C\eta^4 \ , \tag{26}$$

which yields

$$\eta = 0, \qquad\qquad\qquad T > T_c \tag{27}$$

$$\eta = -3B \pm [(9B^2 - 32AC)/8C]^{1/2}, \quad T < T_c \ . \tag{28}$$

The transition temperature in this case is defined as the temperature at which the quantity $(9B^2 - 32AC)$ becomes positive and thus the displacements are real. In the situations which we will be discussing, it will turn out that B may vanish for some displacements and yet be finite for others; thus, there will always be the possibility of both kinds of phase transition.

There are two further items worth noting at this point. The first has to do with the fact that in a first-order transition the symmetry changes discontinuously. The *form* of the free-energy function depends on the symmetry of the crystal. Thus, the transition from the low-symmetry to the high-symmetry phase which depends on the form of the free energy in the low-symmetry phase may occur at a temperature different from the transition from high to low symmetry. Such thermal hysteresis is commonly observed in first-order crystallographic transitions.[25] A second-order transition, on the other hand, in which the free energy changes continuously, will be thermally reversible.

The second point worth noting is the fact that the higher-order terms in the free energy are necessary in order to stabilize the amplitude of the displacements involved in the transition. These terms are related to the third and higher derivatives of the electrostatic potential acting between the atoms in the crystal. Thus, they represent the way in which the interatomic forces change to maintain equilibrium as the atoms are displaced.

With the above general considerations in mind, one would like to move on to a determination of the terms appearing in Φ. The first requirement for this discussion is a more precise description of the atomic displacements. Thus, Landau introduces a density function for the atoms in the distorted phase

$$\rho = \rho_0 + \delta\rho \ , \tag{29}$$

where ρ_0 is invariant under the operations of the high-symmetry space group G_0 and $\delta\rho$ is invariant under the low symmetry G. $\delta\rho$ is assumed to be small and thus must be expressible in terms of the basis functions for the irreducible representations of G_0 which form a complete set of states for small atomic displacements. These functions, of course, are precisely the basis functions determined earlier for the lattice vibrations. Thus,

$$\delta\rho = \sum{}'_{\lambda} \sum_i c_i(\lambda)\phi_i(\lambda) \quad , \qquad (30)$$

where the index λ is used in essentially the same sense as in Eqs. (10)–(18). It is slightly more restricted here, however, in that the index i runs over all of the degenerate phonon eigenfunctions $\phi_i(\lambda)$ transforming according to the space-group representation specified by wave vector $\vec{k}$ and little-group representation m. Thus, $\vec{k}$, m, and a phonon branch label are included in λ while i runs over all of the wave vectors in the star of $\vec{k}$ and over the partners of m, if the representation of the group wave vector has dimensionality greater than one. The prime indicates that the identity representation is to be excluded since it is already present in ρ_0. The phonon basis functions $\phi_i(\lambda)$ are composed of the lattice-dynamic eigenvectors which give the direction and relative magnitude of the atomic displacements involved in a given normal mode. The dimensionless coefficients $c_i(\lambda)$ represent the actual magnitude of the displacement in the $\phi_i(\lambda)$ direction. The free energy then is to be expressed as an expansion in these coefficients $c_i(\lambda)$. The free energy itself must be invariant under the symmetry operations of the crystal. Thus, one can argue for second-order transitions that since the function is continuous across T_c, it must be an invariant of both phases. In particular, it must be an invariant of the higher symmetry G_0. Clearly the operations of the space group transform the basis functions $\phi_i(\lambda)$ into one another without changing the index λ. They can be viewed equivalently, however, as acting on the coefficients $c_i(\lambda)$ while leaving the basis functions fixed. Thus, the $c_i(\lambda)$ themselves form a basis for the irreducible representations of G_0. The free-energy function must then be constructed from linear combinations of products of the $c_i(\lambda)$ which transform according to the identity representation, the Γ^{1+} representation of G_0.

Once again, considerations of stability require that the first term in $\Phi(T, \eta)$ be of second order in the $c_i(\lambda)$. The orthogonality of the irreducible representations of G_0 implies that there is only one such invariant, namely,

$$\eta(\lambda)^2 = \sum_i [c_i(\lambda)]^2 \quad . \qquad (31)$$

Thus, one normalizes the $c_i(\lambda)$ to

$$c_i(\lambda) = \eta(\lambda)\gamma_i(\lambda) \quad . \qquad (32)$$

These new variables $\gamma_i(\lambda)$ possess all the transformation properties of the $c_i(\lambda)$. This order parameter $\eta(\lambda)$ is essentially the same as the one introduced from the lattice-dynamics point of view following Eq. (16). It is slightly more general in that it corresponds to the magnitude of the static displacements along the actual linear combination

of phonon basis functions that best describes the symmetry of the distorted phase. The free-energy expansion is, then,

$$\Phi(T, \eta) = \Phi_0 + \sum_{\lambda} A(\lambda)[\eta(\lambda)]^2 + \sum_{\lambda_1 \lambda_2 \lambda_3} \eta(\lambda_1)\eta(\lambda_2)\eta(\lambda_3)$$

$$\times \sum_{\alpha} B_{\alpha}(\lambda_1, \lambda_2, \lambda_3) f_{\alpha}^{(3)}(\lambda_1, \lambda_2, \lambda_3) + \text{etc.}$$
$$(33)$$

Here $f_{\alpha}^{(n)}$ is an nth-order invariant formed from linear combinations of products of n of the variables $\gamma_i(\lambda)$. There may be more than one such invariant, thus the subscript α. The equilibrium configuration which is determined by the magnitudes of the $\eta(\lambda)$ and the $\gamma_i(\lambda)$ results from a minimization of Φ with respect to all these variables.

It is at this point that group theory comes in handy again, since with it one can determine quickly the number of invariants of a given order, and, in most cases, their actual form. The nth-order products involved in the invariants form a reducible representation whose character is generally equal to the simple product of the characters of the representations involved. Thus, one can use again the character-reduction tables to determine how many times the Γ^{1+} representation will appear in this reducible representation, and thus how many invariants there will be of a given order.

One difficulty arises in the case of invariants formed from basis functions having the same label λ. In such a situation antisymmetric combinations such as

$$\gamma_1(\lambda)\gamma_2(\lambda) - \gamma_2(\lambda)\gamma_1(\lambda) \qquad (34)$$

are null. Thus, one must be careful to use only symmetric combinations for these cases. The reduction of such symmetrized products of representations is also straightforward. Complete tables of the reduction coefficients for direct and symmetrized products of all the representations of O_h^5 are given by Chen, Berenson, and Birman.[23]

Landau, of course, was able to simplify the free-energy expansion considerably by considering the properties of a second-order transition. Such a transition must be determined by the vanishing of a term or terms $A(\lambda)$ at some particular point of pressure and temperature. That more than one of the $A(\lambda)$ should vanish at a particular point, he argued, would be unlikely. That is not to say, however, that several of the $A(\lambda)$ could not vanish at different temperatures and thus give a succession of second-order transitions. For simplicity in discussing a single transition, he restricted the free-energy expansion to displacements transforming according to a single representation, thus,

$$\Phi(T, \eta) = \Phi_0 + \eta^2 A(T) + \eta^3 \sum_\alpha B_\alpha f_\alpha^{(3)}$$
$$+ \eta^4 \sum_\alpha C_\alpha f_\alpha^{(4)} + \text{etc.} \qquad (35)$$

The arguments given above for the case of the second-order transition are now seen to imply that all invariants of third order must vanish identically. This is equivalent to saying in group-theoretical language that the symmetrized cube of the representation in question must not contain the identity representation. Similar restrictions do not exist for first-order transitions; however, it is possible to assert that representations having nonvanishing third-order invariants will give rise to first-order transitions.

At this point it is interesting to look at the relationship between this free energy and that calculated from the lattice-dynamic point of view. The coefficients $c_i(\lambda)$ represent the amplitude of displacement along the phonon basis functions $\Phi_i(\lambda)$. They are thus equivalent to the expectation values of the real normal coordinates $\langle Q(\lambda) \rangle$. In fact, referring back to Eq. (18), we see that Landau's coefficient $A(\lambda)$ is proportional to the square of the temperature-dependent frequency $\omega_T(\lambda)$ of the phonon having quantum numbers λ. Similarly, the other terms in Landau's expansion can be related to the higher-order terms in the expansion of the lattice-dynamic Hamiltonian.[3] The conditions for a second-order phase transition are now seen to imply that the frequency of a single phonon must vanish at the transition temperature. This is the central idea of the soft-mode theory of phase transitions.

Thus, crystallographic transitions from one ordered state to another can be viewed as arising from the temperature dependence of the frequency of one or more phonons. Phonon energies are generally temperature dependent due to interactions between populated states, and to changes in the potential between atoms arising from the thermal expansion of the lattice. What is required here, however, is that the frequency of some normal mode actually approach zero in order to produce a second-order transition.

This interpretation allows us to go even one step further. In the discussion of first-order transitions above, we saw that the requirement for such a transition is the vanishing of the quantity

$$9B^2 - 32AC \quad . \qquad (36)$$

"A" now is the square of the frequency of a particular phonon. Thus, a change in frequency of a phonon can bring about the vanishing of the above expression and therefore a first-order transition. "C" will usually be positive in order to ensure stability against second-order transitions, and

thus even a first-order transition will require a reduction in frequency or softening of some phonon.

The use of lattice dynamics to interpret Landau's theory gives it a much greater range of application than one might have first expected. Of and by itself it could only decide whether or not a given transition involving a particular phonon would be of second order. Now one can see that the discovery of the soft mode or modes of a particular crystal structure may allow the description of all the phase transitions possible from that structure whether of first or second order.

Let us consider first the actual symmetry restrictions imposed by Landau's theory on the phase transitions of fcc R_2MX_6, but with a few physical restrictions in order to keep the discussion finite. We will assume here that such transitions are of second order and that they also preserve inversion symmetry. In addition, Landau demonstrated on the basis of spatial homogeneity that second-order transitions are possible only if the group of the wave vector of the representation under consideration contains within it the operation of inversion. Thus, we are immediately limited to considering representations with wave vectors of the Γ, X, or L points of the Brillouin zone. For these representations of the wave vectors $\vec{k}$ and $-\vec{k}$ are equal within a reciprocal-lattice vector and thus are equivalent. Parity is a good quantum number for such representations. To preserve inversion symmetry we need only consider the representations of even parity, the gerade representations.

A second important physical restriction is that imposed by the x-ray observations to be presented below. These experiments have established that in all the symmetries determined thus far for the distorted R_2MX_6 structure, there are at most four molecules per primitive cell. In addition, none of the structures has reciprocal-lattice vectors with half-integer indices. Thus we can rule out the L-point ($L = \frac{1}{2}, \frac{1}{2}, \frac{1}{2}$) $1/a$ representations from our considerations of possible second-order phase transitions.

In addition, we will be particularly interested in the multiple crystallographic phase transitions that occur in K_2ReCl_6. The sequencing of these transitions is important as far as the discussion at hand is concerned. There is a transition at 110.9 °K which involves no change in the number of molecules per primitive unit cell followed by a transition at 103.4 °K which does involve a change to four molecules per cell. A third transition at 76.05 °K involves no further change in the number of molecules and at one time was thought to result in a low-temperature symmetry of T_h^2. In what follows, we will be trying to describe the two

higher-temperature transitions. Thus, we will concentrate on a transition produced by a Γ-point mode followed by one produced by an X-point phonon.

A quick check of the third-order symmetrized products[23] of the even-parity irreducible representations shows that only the Γ^{4+}, X^{4+}, and X^{2+} can produce second-order transitions. These are the only even representations which do not possess a third-order invariant. To determine the possible symmetries, one has to examine the phonon basis functions for these three representations.

It is at this point that one begins to realize that Mother Nature has been kind. The phonons transforming according to these three representations are unique, i.e., there is only one triply degenerate vibration of each type. One can use the characters of the representations to project their basis functions out of the reducible representation generated by the small displacements of all the atoms. The X^{2+} phonon turns out to be a vibration that involves internal motion of the atoms in the $MX_6^=$ octahedron. This internal mode is known to have an energy of approximately 300 cm^{-1}. Thus, the X^{2+} is an extremely unlikely candidate for the soft mode.

The Γ^{4+} and the X^{4+}, on the other hand, correspond to the longitudinal branch of the rotary mode. The basis functions for the Γ^{4+} consist of solid-body rotations of the octahedra with all octahedra in the crystal rotating in phase. They can be chosen for convenience to be the three orthogonal rotations along the cubic axes, namely, R_x, R_y, and R_z. The X^{4+} is the longitudinal branch of this same rotary mode. Its three basis functions are specified by particular wave vectors from the star of k, i.e., $X_x = (1/a, 0, 0)$, $X_y = (0, 1/a, 0)$, and $X_z = (0, 0, 1/a)$. In the X_x basis function, for example, the octahedra all rotate about the x direction. Those lying in a given plane of the lattice which is oriented perpendicular to the x direction rotate in phase, while those in a plane a distance $a/2$ away also rotate together but out of phase with those in the first plane. It is an "antiferrorotational" basis function composed of ferro sheets which are alternately out of phase.

It is possible that both modes are soft. Thus, we may be able to explain the multiple-phase transitions that are observed by having each approach zero frequency at the appropriate temperature.

What then are the possible symmetries that could be produced by these two modes? Landau does not help us much here since we do not know the magnitudes of the coefficients in the free-energy function and cannot say for sure which linear combinations of the basis functions will minimize it. Since the 110.9 °K transition does not involve a change

in the number of molecules per primitive unit cell, it must be describable in terms of the basis functions of the Γ^{4+} phonon. The possible symmetries are determined by

$$\delta\rho_{110.9\,°K} = \sum_i c_i \vec{R}_i \quad , \tag{37}$$

where $\vec{R}_i$ is one of the three rotations of the octahedra. The space group which leaves $\delta\rho_{110.9\,°K}$ invariant can only be found by inspection of the structure generated by the rotations involved. Note that in such a transition the primitive lattice vectors and the reciprocal-lattice vectors remain the same except for possible minor changes in length. This is due to the fact that all fcc cells distort in exactly the same manner. The resultant symmetries greater than C_{2h} are

$$C_{4h}^5, \quad c_x = c_y = 0, \quad c_z \neq 0 \; ,$$

$$C_{2h}^3, \quad c_x = c_y \neq 0, \quad c_z = 0 \; ,$$

$$C_{3i}^2, \quad c_x = c_y = c_z \neq 0 \quad .$$

The 103 °K transition can be handled similarly, except that it involves a change in the number of molecules per unit cell. The possible third-order invariants within the above symmetries may now be different from those allowed in the fcc symmetry. The dynamics, however, must be essentially the same because of the small displacements. Thus the X^{4+} is still the only phonon capable of producing the transition. The symmetry again must be determined by careful inspection of the structures generated by linear combinations of the X^{4+} basis functions applied to the possible symmetries determined above.

$$\delta\rho = \delta\rho_{103\,°K} + \delta\rho_{110.9\,°K} \quad , \tag{38}$$

where $\quad \delta\rho_{103\,°K} = \sum_i c_i X_i \tag{39}$

and X_i is the basis function transforming as the wave vector X_i.

A single X_i basis function will produce a structure with two molecules per primitive unit cell. There are only two directions of octahedral rotation involved, and therefore, only two types of nonequivalent molecule in the crystal. For an X_z basis function the ferro sheets alternate phase in the z direction. Thus, the unit cell is enlarged in that direction. Calculation of the reciprocal-lattice vectors of the resulting structure shows that X_z is now a reciprocal-lattice vector. The wave vector of the phonon characterizing the distortion becomes a reciprocal-lattice vector of the distorted phase. It is interesting to note that a linear combination of two X_i basis functions produces a structure with four molecules per cell, since the linear combination of the two functions produces four inequivalent directions of octahedral rotation.

In such a situation all three wave vectors in the star of X become reciprocal-lattice vectors of the distorted phase. Similarly, one can see that a transition characterized by an L-point phonon would result in a symmetry in which that L-point wave vector is a reciprocal-lattice vector. The new reciprocal-lattice vectors thus generated would have half-integer indices. The new reciprocal-lattice vectors corresponding to an X-point distortion, on the other hand, have whole integer indices which violate the fcc "all odd or all even" rule. Thus, an x-ray experiment which measures the reciprocal lattice directly can distinguish readily between the two types of distortion.

Figure 4 shows an example of this sort of symmetry construction based on pure rotations of the octahedra. The upper part of the figure shows a Γ-point distortion to C_{4h}^5, while the lower part shows the succeeding X-point distortion to C_{4h}^4 with four molecules per unit cell.

The following lists the possible results of the 103 °K phase transition, assuming that the distortion is characterized by displacements of equal amplitude along one or more X_i basis functions:

$$C_{4h}^5 + X_z = C_{2h}^1 \quad \text{(2 molecules/cell)} \quad \text{(40a)}$$

$$C_{4h}^5 + X_x + X_y = C_{4h}^4 \quad \text{(4 molecules/cell)} \quad \text{(40b)}$$

$$C_{4h}^5 + X_x = C_{2h}^6 \quad \text{(2 molecules/cell)} \quad \text{(40c)}$$

$$C_{2h}^3 + X_z = C_{2h}^5 \quad \text{(2 molecules/cell)} \quad \text{(40d)}$$

$$C_{2h}^3 + X_x + X_y = C_{2h}^3 \quad \text{(4 molecules/cell)} . \quad \text{(40e)}$$

Combinations involving unequal amounts of two or more basis functions generally have only inversion symmetry. The possible phase transitions from the trigonal symmetry C_{3i}^2 have not been enumerated for reasons of brevity.

If one considers the symmetry resulting from these distortions, the number of active phonons predicted group theoretically is larger than predicted by the dynamics of Eq. (17). This is seen by comparison of the representation compatibilities of Table II and the results of Eq. (17) displayed in Table I.

$\vec{R}_z$
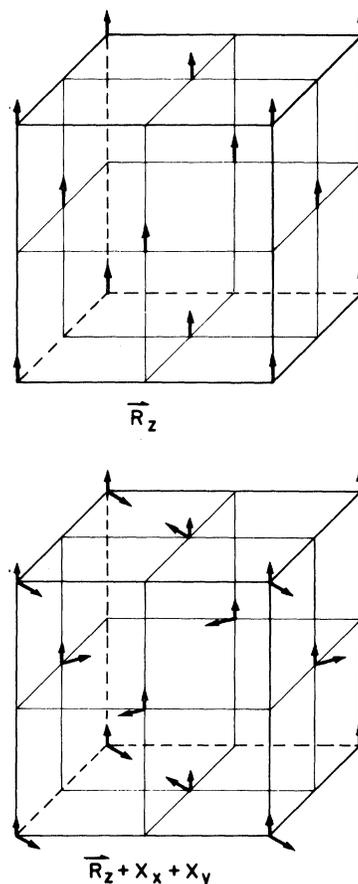
$\vec{R}_z + X_x + X_y$

FIG. 4. Axial vectors denoting sense of rotation associated with each octahedra indicate the crystallographic nature of the phase transitions due to rotational modes whose symmetry is R_z and $R_z + X_x + X_y$.

The third transition at 76 °K is somewhat more of a problem. Since the symmetries of the above analysis are already quite low, we will not attempt any further analysis. It is interesting to note, however, that transitions composed purely of X^{4+} basis functions can have quite high point-group symmetry. In particular, a single X_z function yields D_{4h}^8, while an equal combination of all three

TABLE II. Partial compatibility table for phonons at Γ and at X in O_h^5. E is the time reversed pair.

Symmetry	Representation									Inactive representations	
O_h^5	Γ^{1+} Γ^{3+}	Γ^{4+}	Γ^{5+}	X^{1+}	$X^{2\pm}$	$X^{3\pm}$	$X^{4\pm}$	$X^{5\pm}$			
T_h^2	Γ^1 E	Γ^4	Γ^4	$\Gamma^1 + E$	Γ^4	$\Gamma^1 + E$	Γ^4	$2\Gamma^4$	T_h	Γ^{1-}, E^-	
D_{4h}^6	Γ^1 $\Gamma^1 + \Gamma^3$	$\Gamma^2 + \Gamma^5$	$\Gamma^4 + \Gamma^5$	Γ^2	Γ^4	Γ^3	Γ^1	Γ^5	D_{4h}	Γ^{1-}, Γ^{2+}, Γ^{3-}, Γ^{4-}	
C_{4h}^5	Γ^1 $\Gamma^1 + \Gamma^2$	$\Gamma^1 + E$	$\Gamma^2 + E$	$\cdots$	$\cdots$	$\cdots$	$\cdots$	$\cdots$	C_{4h}	Γ^{2-}	
C_{4h}^4	Γ^1 $\Gamma^1 + \Gamma^2$	$\Gamma^1 + E$	$\Gamma^2 + E$	$\Gamma^2 + E$	$\Gamma^1 + 2\Gamma^2$	$\Gamma^1 + E$	$2\Gamma^1 + \Gamma^2$	$\Gamma^1 + \Gamma^2 + 2E$	C_{2h}	None	
C_{2h}^3	Γ^1 $\Gamma^1 + \Gamma^2$	$\Gamma^1 + 2\Gamma^2$	$2\Gamma^1 + \Gamma^2$	$\cdots$	$\cdots$	$\cdots$	$\cdots$	$\cdots$			
C_{2h}^5	Γ^1 $\Gamma^1 + \Gamma^2$	$\Gamma^1 + 2\Gamma^2$	$2\Gamma^1 + \Gamma^2$	Γ^2	Γ^1	Γ^1	Γ^2	$\Gamma^1 + \Gamma^2$			

gives T_h^2. Thus, the approximate symmetry below 76 °K could be achieved via a single second-order transition from the fcc structure. In fact a second-order transition is also possible from T_h^2 to C_{4h}^4 which is symmetry Eq. (40b). One could possibly consider it as a transition in which the usual temperature order is reversed and imagine a consistent string of second-order transitions which take the salt from O_h^5 straight through to T_h^2. While pathologically interesting, these last considerations will turn out to bear little if any fruit.

Perhaps the most amazing factor of the above analysis is the ease with which the symmetry can be significantly reduced. No mention was made of the actual magnitude of the displacements involved. In fact, the magnitude does not matter in the least. One can start with a rather high symmetry such as O_h^5, and by the addition of a small ferro rotation plus a small antiferro rotation of the octahedra, end up with a structure which would be described as being monoclinic, as in the case of C_{2h} point-group symmetry — all of this with displacements so small that a cursory inspection of a scale model of the structure would lead one to conclude that the symmetry was still fcc. As we shall see later, the experimental determination of such displacements will have to rely heavily on those methods which are most sensitive to the perturbations thus introduced.

To one versed in the literature of phase transitions, perhaps the single most nagging weakness in the above discussion is the continued assumption of second-order transitions. We would like to have some evidence, one way or the other, as to the nature of the particular transitions in question. The specific-heat data which will be reviewed would tend to make one think that all the transitions of K_2ReCl_6 are of second or higher order. It is a skeptical age we live in, however. To be convinced of the nature of the transitions, we must observe directly the continuous change in the order parameter *and* the associated soft mode.

An added concern is the fact that one often sees the words "order-disorder transition"[26] used to describe specific-heat anomalies similar to the ones observed in K_2ReCl_6. Such a transition could arise if the octahedra in the high-temperature phase were not aligned along the cubic-crystal axes, but were randomly rotated by a small amount from the high-symmetry position. This distorted structure could become unstable at some temperature due to the small forces of interaction between the octahedra. The transition, however, would not be driven by a soft mode in the sense in which we have used the term to mean a true phonon involving infinitesimal displacements of the atoms. The successful observation of a soft mode would

argue against an order-disorder transition. We do have some evidence already at hand, however. The very existence of multiple-phase transitions is difficult to explain on the basis of an order-disorder model. Such a model could perhaps explain one transition from a disordered to an ordered state. The remaining phase changes then would involve transitions between ordered states and would be more aptly described by Landau's theory.

We really do need both kinds of information. We need to observe the temperature dependence of the order parameter involved in a particular transition simply to determine its thermodynamic order. And since a continuous behavior of the order parameter is common to both the order-disorder and the Landau type of transition, we would also like to see some evidence for the existence of a soft mode. This evidence has to be carefully chosen, since an ordered system may possess a tunneling type of excitation that exhibits many of the characteristics of a soft mode. The properties of tunneling in the disordered state of such a system are sufficiently different from those of a soft mode as to allow one to distinguish the two. Thus, in what follows, we will be on the lookout particularly for proof of the existence of a soft mode in the high-temperature cubic phase of these crystals.

TEMPERATURE-DEPENDENT STRUCTURE

Ideally a single crystal x-ray study as a function of temperature should allow a complete structure analysis including estimated atom positions, as well as information concerning a long-range order parameter and classification of the thermodynamic order of the phase transitions. In this case of K_2ReCl_6 nature conspired to thwart some of these experimental goals by always forming multiple-domain crystals. The problem, coupled with the very small distortions, made atom-position assignments not unambiguous. Fitting procedures to the x-ray data have shown that the rotation of the octahedra cannot be larger than 2°. However, lattice parameter and the size primitive cell were determined. With the presence of superstructure lines, a long-range order parameter was measured associated with the 103 °K transition. The experimental details of the Dewar defractometer and results of the K_2ReCl_6 structure will be reported more fully elsewhere. Figure 5 shows the lattice constants as a function of temperature, taken on an (8 0 0) reflection from a crystal containing initially two domains in the 103–110.9 °K temperature region. Temperature hysteresis of the 76 °K transition is readily apparent. Hence, one immediately correlates this transition to be thermodynamically first order. In the 76–103 °K
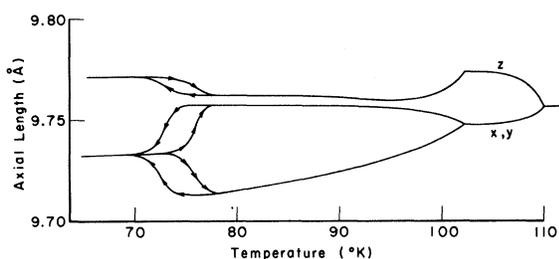
FIG. 5. Axial length as a function of temperature is shown as determined by x-ray diffractometer measurements on single-crystal multiple-domain samples using [800] reflections. Thermal hysteresis is indicated in the 76° transition. Temperature accuracy was approximately 0.1 °K, and relative length accuracy was ±0.001 Å.

region the crystal is clearly of monoclinic or lower symmetry since the three axes have unequal lengths. To within the resolution of the apparatus (0.001 Å), the x and y axes are of equal lengths in the 103–110.9 °K region, implying a tetragonal symmetry. A search was made for the appearance of symmetry-forbidden reflections of the face-centered reciprocal lattices in all temperature ranges. In the range 103–110.9 °K no new reflections were observed, implying the existence of only one molecule per unit cell. In the range 76–103 °K lines of the type $\{2\,1\,3\}$ were observed, indicating that there are four molecules/unit cell. Special efforts were made to observe reflections of the type $\{\frac{1}{2}h\frac{1}{2}k\frac{1}{2}l\}$, without success. Below 76 °K but above 12 °K no new superstructure lines were observed over and above those observed between 76 and 103 °K. Figure 6 shows the integrated intensity as a function of temperature of the superstructure reflection (2 1 3). The intensity is seen to vanish continuously at the 103 °K transition giving credence to the supposition that the transition is second or higher order thermodynamically. For comparison, a similar plot of the (3 5 0) reflection for the K_2SnCl_6 phase transition known to be first order is presented in the same figure.

Expansivity measurements were made with metallic-type strain gauges affixed to crystals along the 110 axis. The results are shown in Fig. 7. One observes a continuous change in expansivity with temperature at the two higher-temperature phase transitions which is consistent with the interpretation of second- and higher-order phase transitions. The 76 °K transition exhibits the hysteresis observed in the x-ray experiments. Finally, associated with the 12 °K transition one also observes a crystallographic distortion as evidenced by the strain-gauge measurements. These results imply not only magnetic but crystallographic ordering at 12 °K. This conclusion is important in that the crystallographic ordering at this tempera-

ture allows an explanation of the temperature dependence of some far-infrared selection rules to be described later.

In summary, these experiments have shown that the 110 °K phase transition is one to a tetragonal symmetry with one molecule/unit cell which is at least of second order, thermodynamically. The 103 °K phase transition is also second or higher order with a monoclinic symmetry involving four molecules/unit cell. The inequivalent molecules are at the fcc sites $0\,0\,0$, $\frac{1}{2}\frac{1}{2}0$, $0\frac{1}{2}\frac{1}{2}$, $\frac{1}{2}0\frac{1}{2}$. The 76 °K phase transition is first order with the same number of molecules/unit cell as the higher-temperature phase. Associated with the magnetic transition at 12 °K we also have detected a crystallographic change whose detailed structure is as yet unknown.

In connection with nuclear quadrupole measurements on the Cl^{35} nuclei in K_2ReCl_6, which were devised to detect the soft mode in the face-centered symmetry, temperature-dependent structure information was also obtained. Since any structure change will be reflected in a change in the magnitude of electric field gradient due to electron dis-
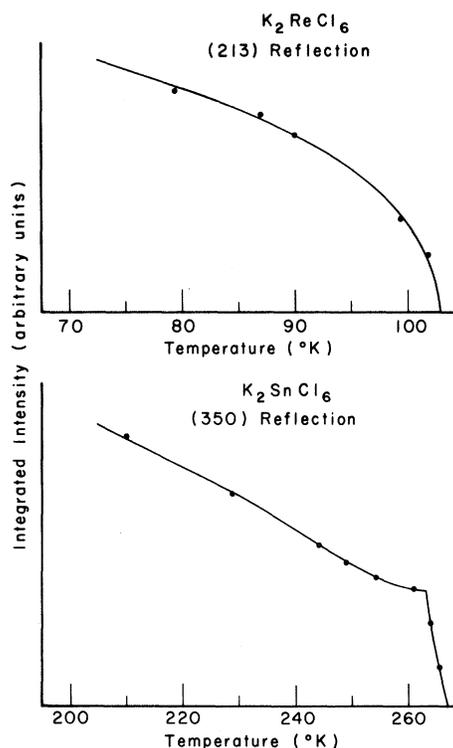
FIG. 6. Long-range order is evidenced by the integrated intensity of super-structure x-ray peaks. (a) Continuous change of the intensity as approaching the phase transition temperature 103 °K suggests a second-order transition in K_2ReCl_6. (b) Abrupt change in integrated intensity for the phase transition in K_2SnCl_6 known to be first order.
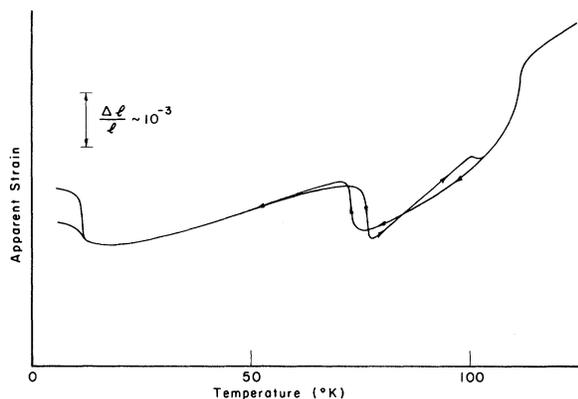
FIG. 7. Apparent strain measured with metal foil gauges as a function of temperature on a crystal of K_2ReCl_6 with the gauge axis along a $\langle 110 \rangle$ crystal direction. Thermal hysteresis is evident at both 12 and 76 °K phase transitions. The apparent thermal hysteresis at 103 °K is due to strains induced by the 76 °K first-order transition. This thermal hysteresis is absent if the sample is not cooled below 76 °K.

tributions at the nuclei, frequency changes reflect differing site symmetries of nonequivalent chlorine nuclei. Figure 8 illustrates the temperature-dependent results. Omitting at this point a discussion of the general trend of increasing frequency with decreasing temperature, these results confirm the interpretation of the x-ray data. In the 103–110 °K temperature region, the ratio of line intensities is 2:1 corresponding to data labeled (x, y) and z, respectively. Thus, within a single octahedron of chlorine nuclei, we associate two types of site symmetries. With the assumption of a rigid octahedra rotating within an environment of cations of tetragonal symmetry, the relative intensities allow us to identify the "z" data with nuclei positioned along the axis and the "x, y" data
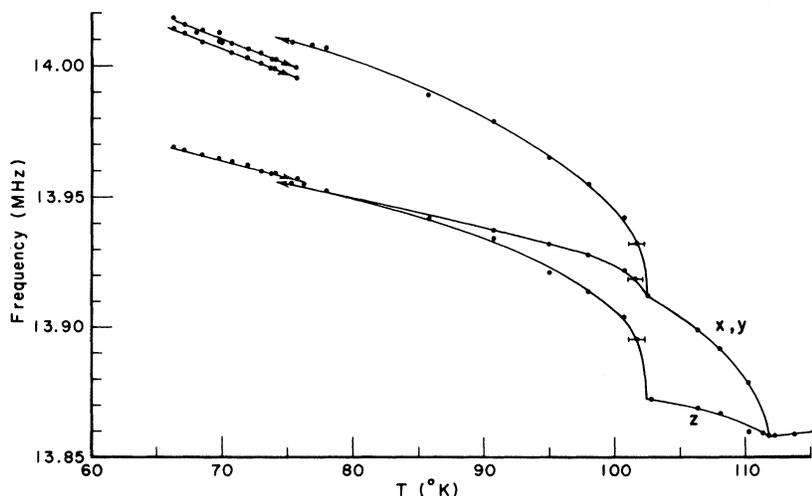
with nuclei positioned in the plane perpendicular to the rotational axis. The data in the intermediate phase again closely follow the lattice-parameter data. Here the relative intensities near 100 °K are equal for all three resonance lines, indicating three nonequivalent pairs of halogen nuclei. As the 76 °K transition is approached from elevated temperatures, two lines coalesce, indicating that two pairs have nearly the same site symmetry. In light of the x-ray superstructure line data, these results are consistent with a monoclinic structure with four molecules/unit cell. The continuous change in frequency with temperature at both the 103 and 110 °K transitions, in contrast to the discontinuous changes occurring at the 76 °K transition, further confirms our identification of the thermodynamic order of the transitions.

The intermediate phase represents a structure with four molecules per cell as identified by superstructure lines corresponding to X points in the fcc Brillouin zone. Hence, the assumptions made in the first section can start to be tested. Since we have seen that the distortion as seen by the chlorine nuclei changes in a continuous fashion approaching the 103 °K transition, and if this transition is due to a soft mode with $k = X$, application of Eq. (17) would predict that to first order the intensity of any phonon mode $Q(\lambda')$ will depend upon the magnitude of the distortion $\eta(\lambda)$ providing the mode $Q(\lambda'')$ is observable in the undistorted phase. First-order perturbation using Eq. (17) gives the intensity of a mode $Q(\lambda')$ to be proportional to the square of the order parameter $\eta(\lambda)$. An example of a far-infrared transition induced by the distortion is illustrated in Fig. 9. The oscillator strength is shown against temperature in Fig. 10, going to zero at 103 °K. We associate this line with observation of $Q(\lambda')$ due to the distortion $\eta(\lambda)$

FIG. 8. Cl^{35} NQR frequency data taken on K_2ReCl_6 below the 110.9 °K phase transition. Experimental error is ±1 kHz and ±0.25 °K except as noted. Evidence for thermal hysteresis is shown in the temperature range about the 76°K transition.
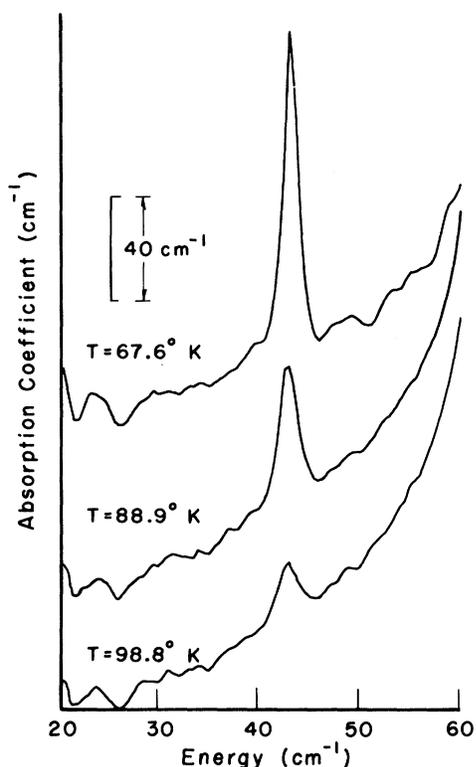
FIG. 9. Infrared spectra of the transverse acoustic node associated with the X point of the fcc zone is shown for three selected temperatures. The energy of this mode is temperature independent from 1.9 to within 0.1 °K of the 103.9 °K phase transition. All infrared spectral data were obtained from an inter-ferometric spectrometer.

where λ' and λ must be equal to the equivalent zone edge points $+X$ and $-X$, respectively. Application of the group-theory selection rules for an X^{4+} distortion with Γ^{4-} (the reststrahlen) as the $Q(\lambda'')$ mode indicates that the line at 43 cm^{-1} must be of X^{5-} symmetry. This clearly can be identified with the transverse acoustic mode at the X point of the zone. The energy of this mode is estimated in a Debye model from the low-temperature specific-heat data of Busey to be approximately 50 cm^{-1}. These infrared data interpreted in light of the structure change at 103 °K confirm the ideas of a distortion of small magnitude. The temperature variation of the oscillator strength, since it changes in a continuous manner, implies that the long-range order parameter likewise varies in a continuous fashion characteristic of a second-order phase transition.

SPECTROSCOPY AND LATTICE DYNAMICS

There remains then the problem of the soft mode. All of the symmetry arguments are based

on it and the very nature of the transitions depends on it. Yet these same symmetry arguments coupled with some independent evidence for the existence of the soft mode will provide the information necessary for the lattice-dynamics calculation. The soft mode itself will provide the all important test of the validity of this calculation with the net result that we will be able to make a rudimentary statement about the forces that are responsible for the phase transitions. We will turn first then to the high-temperature nuclear-quadrupole-resonance (NQR) experiment which yields the necessary proof of the existence of the soft rotary mode in the fcc phase.[27]

It has been suggested recently that NQR may be used to detect the presence of a low-lying librational mode.[28] This possibility arises from the temperature variation of the mean-square nuclear displacement associated with such a mode.

The NQR frequency for a nucleus of spin $I = \frac{3}{2}$ which is located at a crystallographic site possessing axial symmetry is given by $\nu = \frac{1}{2} eQq$, where Q is the nuclear quadrupole moment and q is the zz component of the electric field gradient averaged over the thermal motion of the nucleus. This time averaging comes from the fact that the frequencies of the lattice vibrations are many orders of magnitude higher than the NQR frequency.[29] During one period of precession of the nuclear spin, the nucleus will oscillate many times about its equilibrium position. The gradient will respond essentially instantaneously to the nuclear displacements since it arises primarily from an orientation of the electronic orbitals of the atom in question.
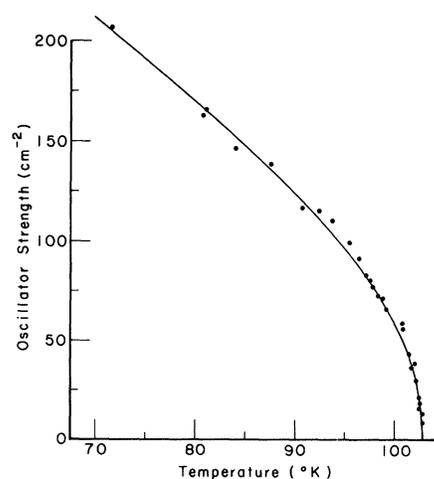
FIG. 10. Oscillator strength of the 43-cm^{-1} transverse acoustic zone-edge mode as a function of temperature. This temperature dependence measures the square of the long-range order parameter as seen from Eq. (17).

The lowest-order nonzero time-averaged term of an expansion of the gradient in the nuclear motion will clearly be proportional to the mean-square displacements. The gradient, and thus the NQR frequency, will vary with temperature according to a weighted Debye-Waller factor involving the motions of the nucleus in question and the atoms which produce the gradient.

The relation between the nuclear motions and the gradient of the electric field is quite complicated in the general case. It simplifies considerably, however, if the following two approximations can be shown to be physically reasonable. The first is the requirement that the major axis of the gradient points toward an origin, another atom, whose equilibrium position lies on the symmetry axis of the nucleus in question. The second is that the dominant thermal motion of the nucleus and the atom at the origin take place in directions perpendicular to the symmetry axis. The lattice vibrational modes which involve motion along the symmetry axis must not be significantly populated at temperatures of interest. The assumption of axial symmetry forces the gradient to be at an extremum for motions perpendicular to the symmetry axis. Thus, the lowest-order effect of such motions will be to rotate the gradient without changing its magnitude.

In this approximation, it is easily shown that the time-average gradient is given to lowest order by

$$q = q_0 [1 - \tfrac{3}{2}(\langle \theta_x^2 \rangle + \langle \theta_y^2 \rangle)] \quad , \tag{41}$$

where q_0 is the gradient in the absence of thermal motion and $\langle \theta_y^2 \rangle$, $\langle \theta_x^2 \rangle$ is the mean-square angle of rotation of the bond axis about the y, x direction.[28,29] Thus, one would ordinarily expect that the gradient and thus the NQR frequency will decrease with increasing temperature due to the normal increase in population of the modes involving rotation of the bond axis. If, on the other hand, the vibration frequency of the dominant rotational mode should increase more rapidly than the temperature itself, the population of that mode would decrease with increasing temperature. This would result in an NQR frequency whose temperature derivative is anomalously positive. Such a rapid temperature variation of the frequency of a rotational mode is just the behavior that is expected above the critical temperature of a soft-librational-mode phase transition.

The chlorine atoms in the fcc phase of K_2ReCl_6 provide an excellent example of a nucleus for which the above conditions are satisfied. Their C_{4v} site symmetry is high enough to force the electric field gradient to be symmetric about the Re-Cl axis. Several pieces of evidence point to the fact that the chlorine is bound covalently to the rhenium

atom. The $ReCl_6^=$ ion is stable in solution. We also know that the internal-mode frequencies of the $ReCl_6^=$ ion are insensitive to the crystalline environment. In addition, the observed magnitude of the NQR frequency can be explained only by assuming that the σ bonding p_z orbital of the chlorine is partially empty.[30]

The final necessary assumption that the vibrational modes involving motion along the symmetry axis be insignificantly populated requires some comment. In the paper by Jeffrey and Armstrong (JA), it is argued that the Debye temperature ($\Theta_D > 200\,°K$) calculated from the specific heat of these crystals is so high that the population of the acoustic mode will be much smaller than that of the low-lying librational mode. We wish to point out here, however, that while their conclusion as to the applicability of the technique is correct, their argument based on population alone is not. In the preceding section it was shown that the zone edge transverse acoustic frequency is only 43 cm^{-1} = 60 °K. The lattice-dynamics calculation which we are about to present will show that the acoustic mode lies *below* the rotary mode nearly everywhere in the Brillouin zone. Thus, in fact, the population of the acoustic mode will be greater than the population of the librational mode. Note that a Debye temperature represents contributions to the specific heat from all the degrees of freedom of the crystal and thus can be considerably higher in energy than the acoustic mode.

One must have some information about the eigenvectors of the normal modes before drawing conclusions about the effect of population. The three internal modes depicted in Fig. 11, which involve a change in the $M - Cl$ bond length, have energies lying between 275 and 360 cm^{-1}.[31,32] These energies are high enough to guarantee small populations of the stretching modes below room temperature. Alternatively, one can say that the acoustic mode involves pure translation of the octahedron as a rigid body. It neither changes the $M - Cl$ bond length nor does it rotate the direction of the gradient. The acoustic mode has no effect on the NQR frequency.

Within these assumptions, the mean-square bending angle of the $M - Cl$ bond including the effects of the molecular bending vibrations as well as those of the rotary mode is the dominant factor in the NQR frequency shift. This angle is given by

$$\langle \theta_x^2 \rangle = \hbar/NR^2 \sum_\lambda |[e_x(Cl|\lambda)/(M_{Cl})^{1/2}]$$
$$- [e_x(Re|\lambda)/(M_{Re})^{1/2}]|^2 \langle n(\lambda) + \tfrac{1}{2} \rangle/\omega(\lambda) \, , \tag{42}$$

where R is the Re-Cl bond length and the other factors are the lattice-dynamic eigenvectors,
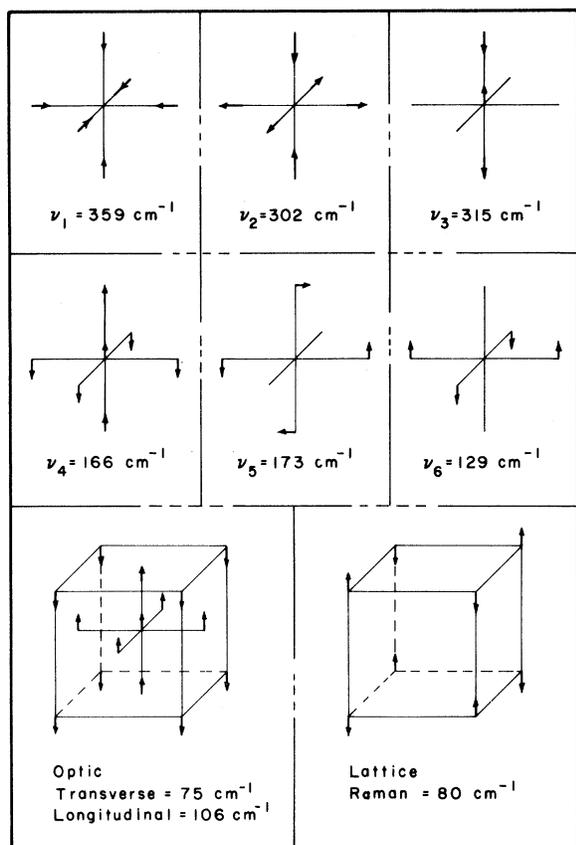
FIG. 11. Schematic representations of the $\vec{k}=0$ modes of the K_2ReCl_6 crystal are indicated together with their observed energies, excluding the octahedra rotary mode. The ν_i modes are the internal modes of the $ReCl_6$ octahedra.

eigenfrequency, and Bose population factor of the λth normal mode. The eigenvectors of the internal modes can be estimated from the requirement that the center of mass of the octahedron remains stationary in the motion. For the rotary mode, the coefficients, exclusive of the population factor and eigenvalues, reduce to $\hbar/I$, where I is the rotational inertia of the $MCl_6^=$ molecule. The population and eigenvalue involve a knowledge of the dispersion of the modes as a function of k. Evidence from optical sideband data will be presented in this section which shows that the dispersion of the three internal bending modes at 126, 166, and 172 cm^{-1} is small enough so that they can be treated adequately as triply degenerate Einstein modes. The contribution of these internal modes is an important one. The combined results of Eqs. (41) and (42) yield an NQR frequency shift of 0.4% at room temperature due to the internal modes alone. This amounts to $\frac{1}{3}$ of the total frequency shift observed by JA in K_2PtCl_6 at room temperature. There-

fore, the contribution of these internal modes is important and should have been included in the analysis by JA. Owing to its dispersion, the rotary mode presents a much more difficult problem of calculation than do the internal modes. The problem is especially acute at low temperatures where the Bose population factor in Eq. (42) must be treated exactly. At high enough temperatures, or equivalently, for low enough rotary-mode energies, the population factor may be expanded as $\langle n(\lambda) + \frac{1}{2} \rangle \cong k_\beta T / \hbar\omega(\lambda)$. In this approximation the NQR frequency shift resulting from the rotary mode will reduce to

$$\Delta\nu_{rot}/\nu_0 = 3k_\beta T/I\overline{\omega}^2 ,$$

where $1/\overline{\omega}^2$ is the average reciprocal square frequency of the transverse and longitudinal branches of this mode.

NQR frequency data taken on K_2ReCl_6 above the transition are shown in Fig. 12. In light of the above discussion of the significant negative-temperature derivative produced by the internal modes, the direct observation of a positive derivative in the raw data indicates the dramatic nature of the temperature dependence of the soft rotary mode. Figure 12 also includes a plot of

$$\overline{\omega}^2 = 3k_\beta T\nu_0/I\Delta\nu_{rot} ,$$

where $\Delta\nu_{rot}$ was determined by first subtracting the calculated internal-mode frequency shift from
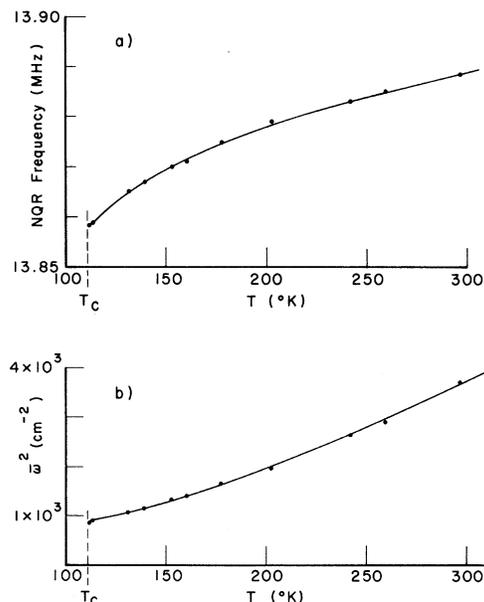
FIG. 12. (a) Raw Cl^{35} NQR frequency data taken on K_2ReCl_6 above the 110.9 °K phase transition. Experimental error is ±1 kHz. (b) Plot of $\overline{\omega}^2$ (see text), with $\nu_0 = 14.050$ MHz determined by extrapolating data taken below the transition to $T=0$ (see Fig. 8).

the raw data. $\bar{\omega}^2$ is very nearly linear in T, and thus, in essential agreement with the classical predictions for such transitions due to Landau. We have indicated that the 110.9 °K transition arises from the softening of the $k = 0$ rotary mode. When account is taken of the small density of states available near $k = 0$, we find that the average frequency $\bar{\omega}$ translates into a $k = 0$ rotary-mode frequency which softens from ~ 25 cm^{-1} at 300 °K to ~ 1 cm^{-1} at 112 °K.

The above interpretation of the high-temperature NQR results in terms of a soft mode can be made more convincing by further consideration of the low-temperature data in Fig. 8. The observation of a negative $(d\nu/dT)_P$ everywhere below the 110.9 °K can be used to argue against several alternative explanations for the high-temperature positive derivative. π bonding has been suggested as a possibility.[30] Optical studies, including optical-sideband of a negative $(d\nu/dT)_P$ everywhere below the 110.9 °K, can be used to argue against several alternative explanations for the high-temperature positive derivitive. ty.[30] Optical studies, including optical-sideband data yet to be presented, have established that the octahedron of chlorines is not distorted in the low-temperature region.[33] Thus, if π bonding were the cause of the anomalous behavior, one would expect to observe positive-temperature derivatives at all temperatures. A second alternative is that the electric field gradient itself might increase with increasing volume,[34] thus producing a positive-temperature derivative of the NQR frequency. This description can be effectively answered by examination of the 103.4 to 110.9 °K temperature region. Because of the tetragonal distortion of the axial lengths and the rigid-body nature of the ReCl$_6$ octahedron, the environment of the x and y chlorines is moving towards them as one goes down in temperature while that of the z chlorine is moving away. This motion corresponds to effective volume expansion for the x and y chlorines and a contraction for the z chlorine as one goes up in temperature. Note that the NQR temperature derivative for the x and y chlorines is, in fact, more negative than that for the z. Thus, the volume dependence does have the normal sign to produce a negative-temperature derivative of the NQR frequency. The volume dependence then is an additional factor to be overcome by the effects of the soft mode which result in the observed negative derivative.

In addition to demonstrating the existence of the soft mode in the fcc phase, the NQR result also allows the elimination of the order-disorder alternative as an explanation for the 110 °K phase transition. In an order-disorder situation, the

amplitude of rotation associated with the tunneling of the octahedra between their equivalent positions is essentially independent of temperature.[26] The rate or frequency of tunneling does change with temperature in much the same way as does the frequency of a soft mode. But since the amplitude is fixed, one will see anomalous effects associated with the transition only when the tunneling frequency gets to be of the order of the quadrupole resonance frequency. For temperatures far away from the transition temperature where the effects of interaction are small, the tunneling frequency can be easily shown to be proportional to the frequency of the true rotational normal mode,[35] and thus is of the order of 10^5 times the NQR frequency. Thus, the actual temperature range in which the two will be comparable is very small. Such behavior is actually observed in connection with magnetic phase transitions. The NQR frequency changes in a normal fashion as one approaches the transition and then suddenly splits into two or more resonances due to the local magnetic fields set up by the onset of long-range order. This is in sharp contrast to the 110.9 to 300 °K range in which the temperature derivative of the NQR frequency of K_2ReCl_6 is anomalously positive.

We are ready to turn then to a detailed examination of the infrared and Raman spectra. The assignments of the vibronic features of the spectra will be of equal importance to the observed frequencies in the process of fitting the lattice-dynamics calculation to the experimental data. It is interesting to look first, however, at the low-temperature spectra to see if there is any evidence for a soft mode in the distorted phases. In fact several features turn out to have marked temperature dependences. Two of these are plotted in Fig. 13. They are the 135-cm^{-1} infrared absorption and the 68-cm^{-1} Raman excitation which ex-
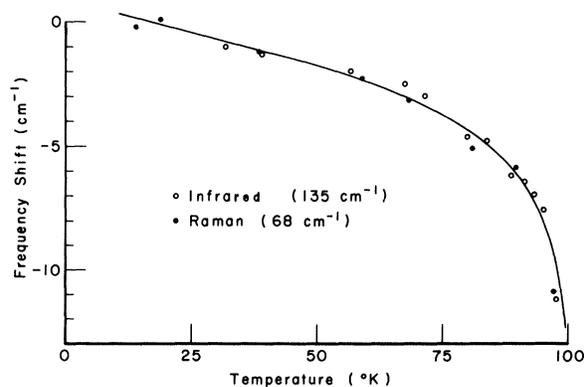
FIG. 13. Frequency shifts of two zone-edge lattice modes as a function of temperature below the phase transition 103 °K.
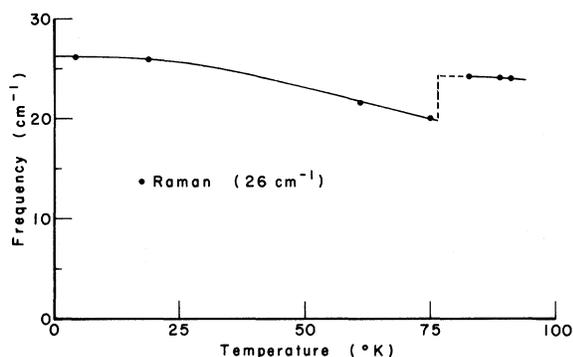
FIG. 14. Raman observed soft Γ^{4+} mode energy as a function of temperature in the distorted phases. Lowest-temperature data point was approximately 6°K, which is below the antiferromagnetic Neel temperature $T_n = 12.1$ °K.

hibit identical frequency shifts as a function of temperature. This behavior coupled with the absence of any infrared reflection anomaly at 135 cm^{-1} strongly suggests that the infrared absorption feature is a two-phonon absorption. In such a process the infrared photon creates two phonons simultaneously. In order to be an electric dipole transition, the phonon basis functions must be of opposite parity. Thus, an infrared process involving the gerade 68-cm^{-1} phonon and some as yet unknown ungerade phonon is a possibility.

The Raman excitation at 26 cm^{-1} (shown in Fig. 14) exhibits a much more marked temperature dependence than do the above-mentioned features. Its frequency changes by nearly 20% between 4.2 and 76 °K. It is also extremely sensitive to the actual symmetry and state of strain of the crystal since it is the only spectrographic feature that is affected by the 76 °K transition. The fact that it is not strongly temperature dependent above 76 °K indicates that it is a possible candidate for the soft mode responsible for the 110.9 °K transition. Thus, it is probably the long sought after Γ^{4+} rotary mode. In addition, an energy of 26 cm^{-1} is not unreasonable in light of the NQR results. It is unfortunate that we were not able to continue to observe this mode above 90 °K. One might expect that it would exhibit quite a dramatic frequency change in the region between 103 and 110.9 °K.

The continued temperature dependence of the 68-cm^{-1} excitation above 76 °K indicates that it is a likely candidate for the soft mode of the 103 °K transition. Thus, it is probably the X^{4+} longitudinal rotary mode.

The above set of identifications is very appealing. We have postulated a model based on a single soft branch of the phonon spectrum, the longitudinal rotary mode in the X direction of the fcc Brillouin

zone. This model consistently describes both of the second- or nearly second-order crystallographic phase transitions that are observed. In addition, we have seen direct evidence for the existence of this soft mode in both the high- and low-symmetry phases and have been able to use the observed temperature dependences to provide a tentative identification and frequency assignment.

Of and by itself, the above evidence is not completely convincing. However, we have not yet brought to bear all of the available spectrographic evidence. It is the totality of the spectral data
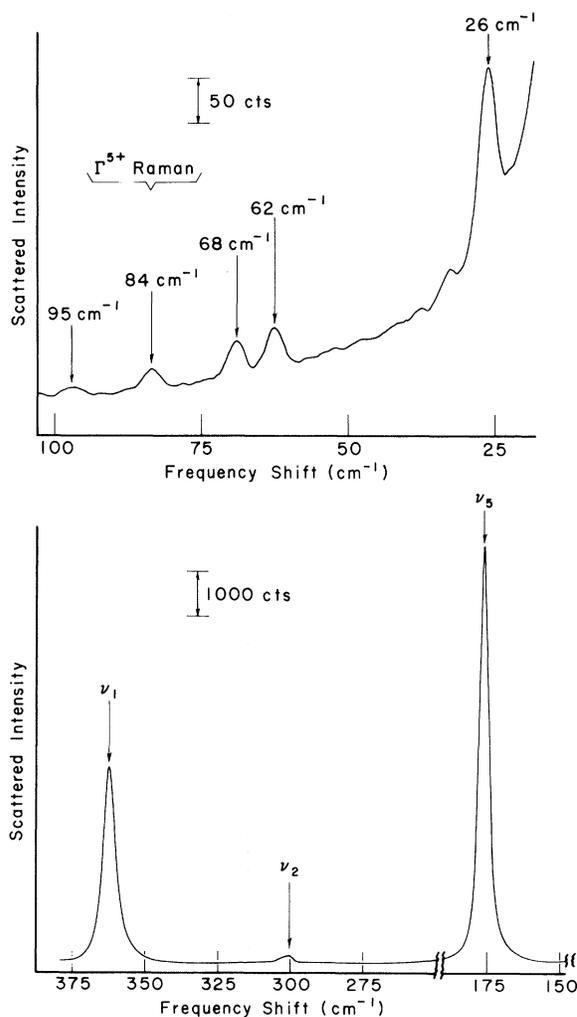
FIG. 15. Raman spectrum at 6 °K of K$_2$ReCl$_6$ taken with argon-ion laser radiation. Internal ν_i modes have energies which are essentially temperature independent. In the fcc structure (above 110.9 °K) only the Γ_5^+ Raman mode is observed shifted to 80 cm^{-1}. Two modes at 95 and 62 cm^{-1} are also temperature independent over the temperature range in which they are observed. See Figs. 13 and 14 for the temperature dependence of the 68- and 26-cm^{-1} lines. The resolution is approximately 2 cm^{-1} for data below 100 cm^{-1}.

coupled with the calculation that will show that our assignments of the soft features are in fact consistent with a dynamic model of the crystal. Thus, we must turn to the rather more mundane business of identifying the features of the spectrum that are not soft.

The Raman spectra taken by Woodward and Ware[31] on ReCl$_6^=$ ions in solution provides the best starting point for the discussion of the fcc Γ-point phonons. Their careful polarization studies allowed the unambiguous identification of the three gerade-type excitations involving internal motion of the octahedra. Our subsequent observation (see Fig. 15) of the same three Raman excitations in solid K$_2$ReCl$_6$ at essentially the same energies then provided further direct evidence for the insensitivity of the internal dynamics of the octahedron to the potassium matrix surrounding it. A fourth Raman excitation of the solid at 84 cm^{-1} could then clearly be assigned to the Γ^{5+} out-of-phase motion of the two potassium atoms. Note that of the low-frequency excitations shown in Fig. 15, only the one at 84 cm^{-1} remains in the fcc phase.

The infrared absorptions can be assigned by comparison with the Raman observations. The similarity of the motion involved in the ungerade ν_3 to that of the gerade ν_1 (Fig. 11) dictates that the 315-cm^{-1} absorption be assigned to ν_3 while the 75-cm^{-1} energy of the transverse optic mode
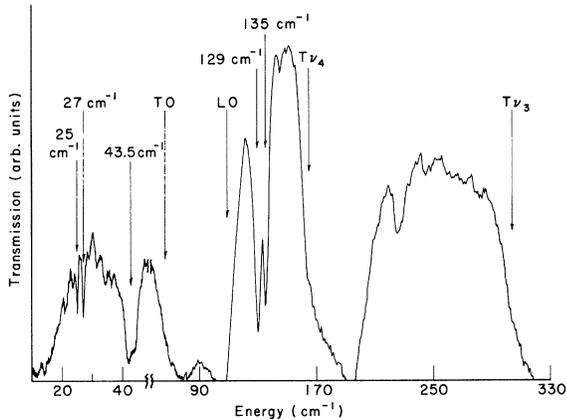
FIG. 16. Infrared spectrum at 1.4 °K of K$_2$ReCl$_6$ obtained with a resolution of 0.5 cm^{-1}. Spectral lines at 25 and 27 cm^{-1} disappear at the antiferromagnetic phase transition. These lines correspond to the Raman observed line at 26 cm^{-1} which is identified in the text with the rotary mode. Since strain gauge measurements (Fig. 7) show that a crystallographic distortion also occurs together with the antiferromagnetic ordering, we may conclude that the resultant symmetry below $T_n = 12.6$ °K does not include inversion. Previous to this study, these lines were incorrectly identified due to their temperature character as magnons.
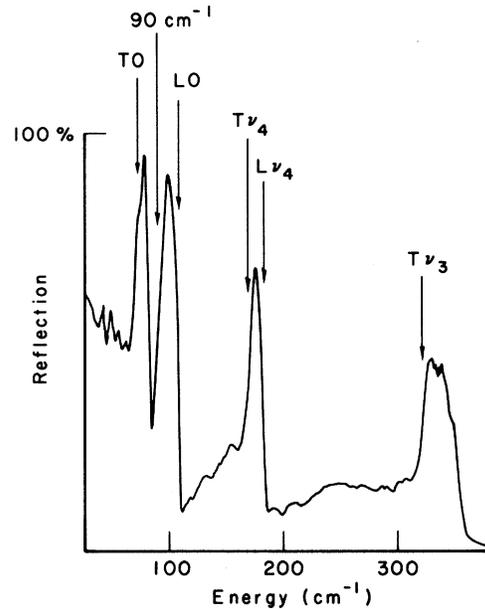
FIG. 17. Infrared reflection spectra of K$_2$ReCl$_6$ at approximately 10 °K. The reflection minima at 90 cm^{-1} disappear in the fcc phase. This anomaly is due to the X^{5-} zone-edge optic mode becoming active due to the distortion. All reflectivity anomalies have energies which are sensibly temperature independent, $\Delta E \sim 1$ cm^{-1}.

clearly indicates its nature. The ν_4 was similarly assigned. The low-temperature infrared-absorption data is shown in Fig. 16. Once again, the optic mode which lies between 75 and 106 cm^{-1} is the only low-energy feature that remains in the high-temperature fcc phase. The additional degrees of freedom supplied by the electromagnetic field in an ionic crystal result in a splitting of the Γ^{4-} phonons into two modes, one of which is doubly degenerate and polarized transversely, while the other is polarized longitudinally to the wave vector of the phonon. As is well known, the presence of these modes results in an infrared stop band between the transverse and longitudinal frequencies. The transverse and longitudinal frequencies of the three infrared active phonons were determined from the reflection data shown in Fig. 17. The regions of near perfect reflection are bounded by the transverse and longitudinal frequencies of each mode.

These assignments and measured energies, along with a schematic representation of their basis functions, are shown in Fig. 11 for phonons of zero wave vector. The ν_6 vibration was observed as a sideband of a transition to an excited Γ_7 electronic state of the rhenium atom. The sideband data will be discussed later in relation to the lattice-dynamics calculation of phonon energies of arbitrary wave vector.

The discussion presented in the theoretical section dealing with the perturbation Hamiltonian [Eq. (17)] for a slightly distorted crystal provides the basis for the assignment of the new spectral features that appear in the low-temperature regions. We now know that the 110.9 and 103 °K transitions are characterized by Γ^{4+} and X^{4+} distortions, respectively. Table I has already presented the theoretical conclusions as to which phonons would be expected to become strongly active in the presence of these distortions. At the 110.9 °K transition one expects both silent Γ- point modes, the Γ^{4+} and the Γ^{5-}, to become strongly active. At the 103 °K transition the lattice modes which will become strongly active are the X^{4+}, X^{5+}, and X^{5-}. Thus, in the infrared, we expect to see the X^{5-} transverse acoustic mode and not the X^{4-} longitudinal acoustic. This is in accord with our previous assignment of the 43-cm^{-1} absorption via the Debye temperature arguments. We would also expect to see the X^{5-} transverse mode involving potassium motion. The only other strong infrared feature in the lattice-mode region of the spectrum is the reflectivity dip at 90 cm^{-1} which can be seen in Fig. 17. Thus, we assign it to this X^{5-} phonon.

The Raman data which were shown in Fig. 15 can be analyzed similarly. We have already tentatively identified the excitations at 26 and 68 cm^{-1} as belonging to the longitudinal branch of the rotary mode at $\vec{k} = 0$ and $\vec{k} = \vec{X}$, respectively. These are the Γ^{4+} and the X^{4+} modes which according to the above analysis should be strongly active in the distorted phases. Clearly then, the two excitations at 95 and 62 cm^{-1} must be the two X^{5+} modes. A final statement as to which is which will have to wait for the results of the calculation.

As was pointed out previously, the similarity of the temperature dependence of the 68-cm^{-1} Raman excitation with that of the 135-cm^{-1} infrared absorption leads one to conclude that the 135-cm^{-1} mode is a combination of the 68-cm^{-1} phonon with some phonon having an energy of 67 cm^{-1}. The basic requirement for such a combination band-type of absorption is that the product of the representations involved contains the electric dipole Γ^{4-} representation. One can always obtain a product that contains Γ-point representations by considering phonons of equal and opposite wave vector. Thus, the phonons visible in such a process are not restricted to long wavelengths. In this particular case then, the 67-cm^{-1} phonon that we need must also transform according to an X-point representation. Referring again to Birman's tables of products of representations,[23] we see that any of the ungerade phonons at X will work. The only two ungerade lattice phonons that remain to be assigned are the X^{2-} (potassium motion) and the X^{4-}

(longitudinal acoustic). The optical sideband data which we are about to consider will show us that the X^{2-} is the most likely candidate.

Thus, we have succeeded in producing a no-calculation positive identification of one new phonon at the X point, the X^{5-} potassium motion mode, and have reconfirmed our previous assignments of the rotary and transverse acoustic modes. Before proceeding to the actual calculation, let us look at one last piece of data, the optical sidebands.

The three unpaired electrons in the $5d$ shell of the rhenium atom possess an excited state at 13 896 cm^{-1} which transforms as the cubic double-group representation Γ_7. The transition between the ground electronic state which is a Γ_8 and this one has been verified to be a purely magnetic dipole transition.[33] The slight splitting of this excited state which appears to the far left of the optical-absorption spectrum shown in Fig. 18 is due to the presence of local magnetic fields arising from the antiferromagnetic ordering. The data was taken at 1.5 °K.

Simultaneously with the electronic excitation, the optical photons can also create lattice-vibrational phonons. It is these phonon sidebands that give rise to all the gross features of the optical data. These sidebands are electric dipole transitions. Thus, as in the case of the phonon combination bands observed in the infrared, the product of representations involved must contain the Γ^{4-} representation. In order to take these products correctly, one must treat the electronic transition as a true elementary excitation of the crystal, i.e., as an exciton with energy and momentum eigenvalues. Thus once again, momentum conservation
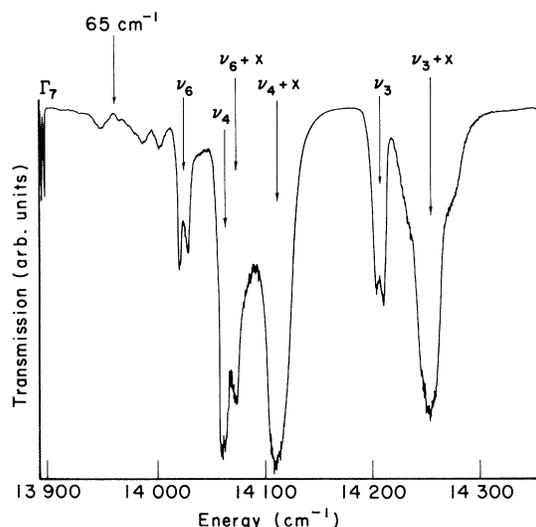
FIG. 18. Optical sideband data of K_2ReCl_6 at 1.4 °K obtained with a Bausch and Lomb 1-m spectrograph with a resolution of less than 0.5 cm^{-1}.

with the incident photon can be satisfied by considering phonons and excitons of equal and opposite wave vector. The fact that the sideband phonons may be of nonzero wave vector will turn out to account for the differences between this and the true $\vec{k} = 0$ data and will also give us some new information that was not available in the Raman and infrared spectra.

At this point then we must look more closely into the real nature of the sideband transitions. The pure electronic transition is by its very nature a localized excitation. Its energy is determined almost entirely by the crystal field generated by the octahedron of chlorine atoms surrounding the rhenium atom in addition to spin orbit and electronic effects which are internal to the atom itself. Thus, the energy of the exciton associated with this electronic level is essentially independent of its momentum.

In the vibration sidebands, the distortion of the octahedron produced by the phonon created an essentially static change in the crystal field seen by the rhenium atom. This change is static because of the very low frequency of the phonon in comparison with the energy of the electronic transition. If the phonon-induced distortion is of a local ungerade nature, it will generate odd terms in the crystal field which will mix electronic configurations of opposite parity into the ground and excited states. It is this parity difference that gives the sidebands their electric dipole character.

The most important feature of this discussion is that fact that the excitations are localized. They involve the transition of a single electron on an atom to an excited state perturbed by a local distortion of the crystal field in which that atom sits. The distortion is assumed to have only a very small effect on the energy of the electronic state. Its major effect is felt in first order in the eigenfunctions of that state and, thus, in the type of transition that is observed. Since the distortion is localized, the phonons that generate it must also be of a local nature. The spatial extent of an excitation is related to its extent in momentum space via a Fourier transform. Thus, the wave vectors of the sideband phonons will be spread over the entire Brillouin zone. The shape of the optical sidebands thus reflects the density of states in energy for the normal modes which distort the octahedron. This density is highest for modes of short wavelength. Thus, the absorption peaks correspond to phonon energies near the edge of the Brillouin zone.

The three sharp features at 129, 166, and 312 cm^{-1} correspond to the ν_6, ν_4, and ν_3 internal modes, respectively. The narrow linewidth of these absorptions indicates that the dispersion of the internal modes is quite small, substantiating our earlier statement. The energies observed here for the ν_4 and ν_3 modes also agree quite well with the frequencies obtained from the far-infrared absorption data (Fig. 16). The identification of the ν_6 phonon was obtained thanks to a calculation by Krynauw and Pistorius[36] of the energies of the internal modes of the $ReCl_6^-$ molecule. In addition, the small splittings of these three features can be interpreted as being due to the slight differences in energy between the transverse and longitudinal branches of these modes at the zone edge. Thus, the optical data yield quite a bit of new information about even the internal modes. We have here a total of six zone-edge frequencies for the ungerade internal modes.

The broad features below 120 cm^{-1} give a weighted density of states of the lattice modes. As we have indicated above, the intensity of a given sideband depends on the size and type of crystal field change produced by the phonon in question. Thus, a complete identification of all the low-lying sideband peaks is beyond the scope of this work. It would require not only a knowledge of the phonon basis functions throughout the Brillouin zone, but also an explicit model for the mechanisms which produce the crystal field. We can say with some certainty, however, that the peaks between 65 and 110 cm^{-1} correspond to the optic and Raman active modes, while those below 65 cm^{-1} arise mainly from the acoustic mode. The rotary mode does not distort the octahedron and, thus, is not visible. The absence of any features in the region around 65 cm^{-1} indicates that there is probably a gap in the spectrum exclusive of the rotary mode. The dispersion curves of the acoustic and the optic modes do not overlap in energy. This implies that the longitudinal acoustic mode lies below 65 cm^{-1} at the zone edge and, thus, that the unknown ungerade mode responsible for the 135-cm^{-1} two-phonon infrared absorption must be the X^{2-} phonon. The X^{2-} is the zone-edge longitudinal branch of the Γ^{5+} Raman-active mode.

The three strong peaks at 175, 210, and 360 cm^{-1} do not correspond to any of the ungerade internal modes. These energies can be written consistently as $\nu_6 = x = 175$ cm^{-1}, $\nu_4 + x = 210$ cm^{-1}, and $\nu_3 + x = 360$ cm^{-1}, where $x = 50$ cm^{-1}. Thus, it is not unreasonable to assume that they are two-phonon processes. Their breadth indicates the second phonon which is common to the three peaks must be a lattice mode. Incidentally, their breadth also rules out the possibility of their being internal modes. The most likely candidate for this second phonon is the longitudinal acoustic mode at or near the zone edge.

Perhaps it would be wise to stop and review the knowledge that we have gained up to this point.

Thanks to a fortuitous phase transition, we have been able to observe and identify a large number of phonons, many of which would normally be accessible only through inelastic neutron-diffraction techniques. In fact, if we stop and count up all the transitions tentatively identified thus far, we find that we have a total of 22 known phonon energies. These are all collected together and shown in Table III. Out of this total number we are certain of the basis functions of 14 if we include the rotary mode. The remaining 8 energies have a twofold ambiguity. In the case of the internal modes, this uncertainty is between the transverse and longitudinal modes at the zone edge while in the Raman data it lies in the assignment of the two X^{5+} modes. In addition, the sideband data have shown us that the longitudinal acoustic mode at the zone edge lies below 65 cm^{-1}.

We are going to proceed then to fit these energies to a model that will involve 13 independent parameters. If we did not know the eigenfunctions of a large number of these, this would certainly be a chancy business. The knowledge of the eigenfunctions that we do have, however, is more than sufficient. In fact, we have enough information so that we can be quite honest in the fitting and ignore that which is controversial, namely, the rotary-mode assignments. The lattice-dynamics calculation will turn out to give reasonable values for the rotary-mode energies without any attempt to force it to produce the observed values.

As was mentioned previously, we will use a rigid-ion model in which the forces acting between the atoms can be broken down into a long-range Coulomb part due to the ionic charges and a short-range part due to the actual overlap of the electron distributions of neighboring atoms. One must exercise some care in calculating the Coulomb contributions to the dynamic matrix,

$$D_{\alpha\beta}^{(C)}(k; n, n') = \sum_l [1/M_n M_{n'})^{1/2}] \exp[-2\pi i \vec{k} \cdot \vec{X}(l)]$$

$$\times \frac{\delta^2[\vec{X}(l, n') - \vec{X}(0, n)]^{-1}}{\delta X_\alpha(0, n)\delta X_\beta(l, n')} q_n q_{n'} \quad , \tag{43}$$

where q_n is the ionic charge on the nth atom in the unit cell. This sum can be evaluated numerically by using Ewald's method,

$$\sum_l \exp[-2\pi i \vec{k} \cdot \vec{X}(l)]/|\vec{X}(l) - \vec{x}|$$

$$= 1/(\pi V_c)\sum_K \exp[2\pi i(\vec{K} - \vec{k}) \cdot \vec{x}]$$

$$\times \exp[-\pi^2 |\vec{K} - \vec{k}|^2/G^2]/|\vec{K} - \vec{k}|^2$$

$$+ \sum_l \exp[-2\pi i \vec{k} \cdot \vec{X}(l)]$$

$$\times \mathrm{erfc}[G|\vec{X}(l) - \vec{x}|]/|\vec{X}(l) - \vec{x}| \quad . \tag{44}$$

TABLE III. Observed and calculated low-temperature energies.

Mode	How observed	Observed energy	Calculated energy (Model I)
Γ^{4+} rotary	I. R., Raman	26 cm^{-1}	45.2 cm^{-1}
X^{4-} TA	I. R.	43[a]	36.7
X^{5+}	Raman[b]	62	63.5
X^{2-}	I. R. (2 phonon)	67	70.9
X^{4+} rotary	Raman	68	70.2
Tran. optic	I. R. (trans. and refl.)	75[a]	77.0
Γ^{5+}	Raman	84[a]	84.9
X^{5-}	I. R. (reflection)	90	92.8
X^{5+}	Raman[b]	95	96.3
Long. optic	I. R. (trans. and refl.)	106[a]	104.9
ν_6 zone edge	Sidebands[b]	122[a]	122.5
ν_6 zone edge	Sidebands[b]	129[a]	129.6
ν_4 zone edge	Sidebands[b]	164[a]	158.8
ν_4 zone edge	Sidebands[b]	166[a]	166.8
Tran. ν_4	I. R. (trans. and refl.)	166[a]	168.4
ν_5	Raman	172[a]	171.6
Long. ν_4	I. R. (reflection)	180[a]	179.4
ν_2	Raman	302[a]	300.8
ν_3 zone edge	Sidebands[b]	307[a]	307.6
ν_3 zone edge	Sidebands[b]	313[a]	312.0
Tran. ν_3	I. R. (trans. and refl.)	320	316.7
ν_1	Raman	359[a]	359.6
X^{4-}LA	Sidebands	≤65[a]	66.4

[b] Indicates twofold ambiguity.
[a] Energies used in fitting Model I.

In this expression the slowly converging Coulomb sum has been broken up into two rapidly converging sums. The first is over reciprocal-lattice vectors $\vec{K}$ and the second is over the direct lattice vectors $\vec{X}(l)$. The number G is chosen in such a way as to make both sums converge to approximately 0.1% accuracy when they are taken over a sphere centered at $\vec{k}$ or $\vec{x}$, as the case may be, and having a diameter of 2.5 times the nearest-neighbor distance. Having this convergent expression for the sum, one can easily differentiate it term by term to obtain the dynamic matrix. One must be careful to exclude the self-energy term in which $\vec{X}(l, n') - \vec{X}(0, n) = 0$. In addition, one must take the limit as k approaches zero correctly, since after differentiation the term in the first sum with $\vec{K} = 0$ will have different limits depending on the direction of $\vec{k}$. It is just this difference in the values of the limits that will give rise to the difference in energy between the transverse and longitudinal infrared active modes at $\vec{k} = 0$.

Symmetry requires that the six chlorines have the same effective charge and similarly for the two potassium charges. In addition, the crystal must be electrically neutral, thus

$$2q_K + q_{Re} + 6q_{Cl} = 0 \quad . \tag{45}$$

There are then only two independent charges to be

used as parameters. These will be taken to be the rhenium and chlorine effective charges.

The short-range forces will be assumed to arise from central potentials acting between the atoms:

$$U(0, n; l, n') = U[\,|\vec{X}(l, n') - \vec{X}(0, n)|\,] \quad .$$

The derivatives that are needed are then easily calculated in terms of the derivatives of this potential with respect to $R = |\vec{X}(l, n') - \vec{X}(0, n)|$.

$$U_\alpha(0, n; l, n') = R_\alpha / R\, U'(R) \quad ,$$

$$U_{\alpha\beta}(0, n; l, n') = \frac{1}{R}\, U'(R)\left(\delta_{\alpha\beta} - \frac{R_\alpha R_\beta}{R^2}\right)$$

$$+ \frac{R_\alpha R_\beta}{R^2}\, U''(R) \quad . \tag{46}$$

Thus, there are two independent parameters for each pair of atoms that interact via short-range potentials. These are the first and second derivatives of the potential which are generally referred to as the perpendicular and parallel force constants, respectively. The stability condition

$$\sum_{l, n'} U_\alpha(0, n; l, n') = 0 \tag{47}$$

further reduces the number of independent parameters by one, since it vanishes by symmetry for all but the chlorine atoms.

The actual model that is used involves detailing the pairs of atoms that are assumed to interact most strongly via short-range forces. In Fig. 19 the atoms in the unit cell are numbered for easy reference in this discussion. With the exception of the Re-K pair, all of the atoms in the unit cell are assumed to interact with one another and with all other symmetry-related atoms. Symmetry-related pairs will all interact with the same force constants, thus providing a tremendous reduction in the number of independent parameters. For example, Cl 6 and K 8 will interact with the same force constants as will Cl 4 and K 9, and K 8 will interact via the same force constants with a total of six K 9-type atoms, one of which is in the unit cell at the origin and the remainder being in the neighboring unit cells. There result, then, five independent pairs of atoms within the unit cell. In addition, one must take into account the interactions between the Cl atoms on neighboring octahedra since some of these are separated by distances that are of the order of the separations between chlorines on a single octahedron. These interunit cell pairs are not related by symmetry to any of the intraunit cell pairs and, thus, will have independent force constants. Only two such pairs are included in the model. These are the Cl 3 in the cell and the origin to Cl 2 in the ($\frac{1}{2}a, \frac{1}{2}a$, 0) unit cell and the Cl 3 (0, 0, 0) to Cl 5 ($\frac{1}{2}a, \frac{1}{2}a$, 0) force constants.

Thus, we have taken account of the short-range

potentials acting between all atoms that are closer to one another than approximately one-half the side of the simple cubic unit cell. This amounts to seven independent pairs of atoms with two force constants each plus the two charges for a total of 16 parameters. The stability condition given above reduces the number of independent first derivatives or perpendicular force constants by one. This condition is nothing more than the requirement that the Re-Cl distance should be an equilibrium separation. Remember that the Cl$^-$ position is not determined completely by symmetry as is the case for the Re^{4+} and K$^+$ ions.

There is one further stability condition that can be used. In addition to the above requirement that each atom be in equilibrium, we would also like the observed lattice constant to be an equilibrium value. This condition can be stated in two alternate ways. The first is to say simply that the crystal must be in a state of vanishing stress, which is to say, in a sense, that the total pressure produced by the interaction of one unit cell with all its surroundings must vanish. The second point of view is that the crystal must be stable against isotropic expansion or contraction. Cubic crystals are stable against shear-type deformations by virtue of symmetry. In an isotropic deformation, the displacement of a given atom in the crystal is proportional to its distance away from the origin. Thus, such a deformation will make a contribution to the total potential energy of the crystal that is proportional to

$$\sum_{\alpha, l; n, n'} R_\alpha U_\alpha(0, n; l, n') = \sum_{\alpha, l; n, n'} R_\alpha^2 U'(R)/R \quad . \tag{48}$$

FIG. 19. Local environment of the ReCl$_6^=$ octahedron in the fcc crystal K$_2$ReCl$_6$.

FIG. 20. Dispersion curves for the internal modes calculated from model I indicating symmetry labels and all mode energies deduced from the spectral data.

For stability then, this contribution which would be linear in such a deformation must also vanish. Thus, we have a second condition on the perpendicular force constants and one less independent parameter. In actual practice this last condition was taken account of in an approximate fashion by applying it only to the forces acting between the octahedra. This was done so that small errors in the internal mode frequencies would not dominate the interoctahedra force constants via the relationship set up by this condition.

In the process of fitting it turned out that the first derivative of the potential between the two potassium atoms was so small as to be indeterminate. Thus, it was to set to zero and not used as a parameter. We end up then, after ignoring this

one force constant and taking account of the two stability conditions, with a total of 13 parameters which were used to fit the 16 energies indicated in Table III. These 16 energies were the ones of which we felt most sure at the time.

The results of the least-squares fit shown in Table III are also in Figs. 20 and 21. We refer to the results of this fit to 16 energies as model I. The parameters of this model are given in Table IV. The rms deviation for all the observed levels exclusive of the Γ^{4+} rotary mode is 2.4 cm^{-1}. This remarkable agreement with all of the levels, including six that were not used in the fitting procedure, is extremely encouraging. The agreement, coupled with the fact that the model produces a crystal that is stable, is a very convinc-
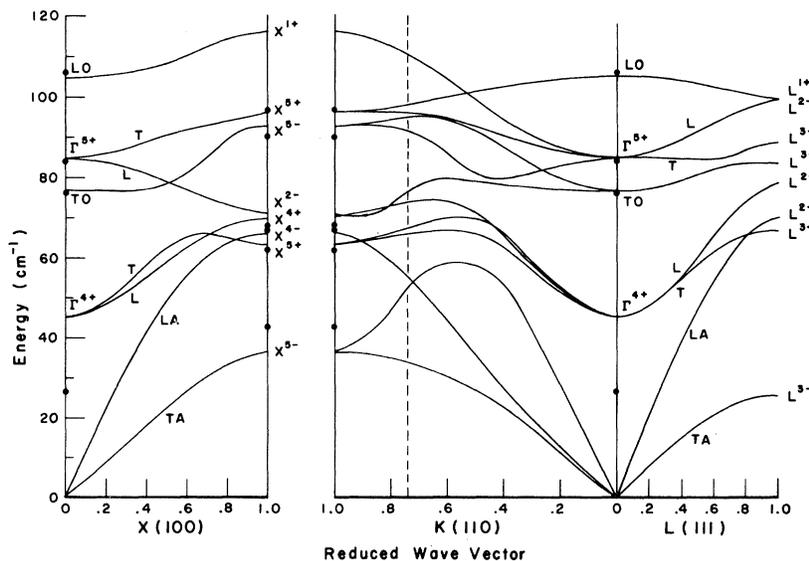
FIG. 21. Dispersion curves for the lattice modes calculated from model I indicating symmetry labels and all mode energies deduced from the spectral data.

TABLE IV. Lattice dynamics parameters.[a]

Parameter		Model I		Model II	
Charges					
Re		0.40e		0.38e	
Cl		− 0.32e		− 0.32e	
K		0.76e		0.78e	
Force constants	Parallel	Perpendicular		Parallel	Perpendicular
Cl3$(0,0,0)$-Cl4$(0,0,0)$	0.15(mdyn/Å)	− 0.027(mdyn/Å)		0.16(mdyn/Å)	− 0.025(mdyn/Å)
Cl3$(0,0,0)$-Cl4$(\frac{1}{2},-\frac{1}{2},0)$	0.063	0.0027		0.065	0.0016
Cl2$(0,0,0)$-Cl4$(0,0,0)$	0.31	− 0.020		0.30	− 0.026
Cl2$(0,0,0)$-Cl4$(\frac{1}{2},-\frac{1}{2},0)$	0.0067	− 0.015		0.0029	− 0.015
Cl3$(0,0,0)$-K8$(0,0,0)$	0.067	− 0.011		0.068	− 0.012
K8$(0,0,0)$-K9$(0,0,0)$	0.0066	0		0.0075	0
Re1$(0,0,0)$-Cl4$(0,0,0)$	1.31	0.14		1.30	0.14

[a]Charges are expressed in terms of the (positive) electronic charge e. Force constants are expressed in units of millidynes per angstrom. = mdyn/Å. mdyn/Å = 10^5 dyn/cm.

ing argument in favor of the assertion that this model does produce a reasonable description of the dynamics of this crystal structure.

But what of the rotary mode? In this model it has an energy of 45 cm^{-1}, whereas our low-temperature observed energy is 26 cm^{-1}. We must remember, however, that the calculation was done for the cubic symmetry using the room-temperature lattice constant. If this mode is really the soft mode of the 110.9 °K transition, as we have been postulating, then its frequency must be very sensitive to the actual lattice constant and also to the crystallographic symmetry. Thus, we would not expect precise agreement with the energy observed in the low-temperature phase. The simple fact that the Γ^{4+} energy is small and that the X^{4+} energy does agree with the observed value is very encouraging, however.

We have one basic experimental fact left at our disposal, namely, the rotary mode is observed to move while the rest of the phonon energies are essentially independent of temperature. Thus, if the model is a reasonable one, it should be able to reproduce this behavior. In order to test this hypothesis, the fitting procedure was repeated but with the observed rotary-mode energy of 26 cm^{-1} included as one of the points to be fitted.

The results of this calculation are extremely gratifying. The rotary mode can be moved by relatively large amounts while holding the other energies fixed. These results are shown in Fig. 22, and the parameters of this fit, model II, are given in Table IV. In addition, the longitudinal rotary X^{4+} mode also moves down while the transverse branch is unaffected. This corresponds to the observed motion of both modes. The longitudinal rotary mode in the X direction moves more than does the rotary mode at the other zone-edge points. This agrees with the fact that only X- and Γ-point phase transitions are observed. The

shape of the rotary-mode dispersion also suggests that a transition from the fcc structure which involves the X^{4+} mode would probably be of first order, since it would be difficult for this mode to get to zero before the Γ^{4+} mode does so. This confirms our previous conclusion based on Landau's theory that the transition of K$_2$SnCl$_6$ must be of first order. It does not rule out, however, the possibility that an X-point transition which follows a Γ-point second-order transition might also be of second order. This is due to the fact that the Γ-point distortion will cause the Γ^{4+} energy to rise below the transition. Thus, the X^{4+} energy may continue on towards zero at some lower temperature.

Our final point is worth making. The above fitting procedure for moving the rotary mode is an attempt to simulate the lattice contraction and other anharmonic effects by changing the force constants while holding the lattice fixed. Examination of the force constants given in Table IV for the two mod-
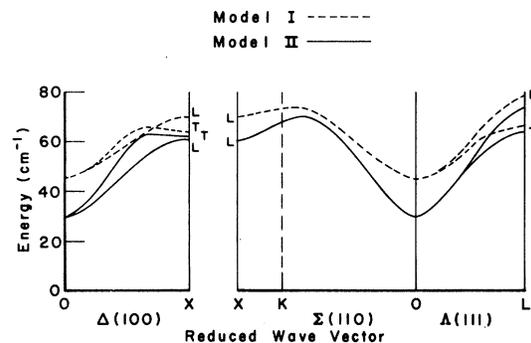
Model I ------
Model II ———

FIG. 22. Dispersion curves for the rotary mode calculated for both model I and model II. The labels L and T refer to the longitudinal and transverse branches, respectively. Interestingly, in collaboration with observation, the longitudinal mode at the zone edge is much softer than the transverse mode.

els shows that the magnitude of the changes required to produce the shift in the rotary mode is quite small. In addition, the parameters most strongly affected are the force constants which act between Cl^- ions on neighboring octahedra. The one constant internal to the octahedra which does show a change is a reflection of the enforced lattice stability combined with the fixed lattice constant. A fit of these short-range parameters to a Lennard-Jones "six-twelve" potential shows that such force-constant changes are possible as a result of a typical lattice thermal contraction (approximately 0.2% in 100 °K). The limited nature of the nearest-neighbor rigid-ion model prevents one from making an extensive attempt at a physical interpretation of the parameters.

It does appear, however, that the soft mode in these salts arises purely from changes in the short-range force constants. An alternative way of saying this is that the interactions which produce the phase transitions are of a very local character. At some later date perhaps it would be worthwhile to attempt to construct a more physical model for these interactions. Such an attempt is beyond the scope of this work.

CONCLUSION

Thus, we have come to the end of the road as far as the information available at this time is concerned. Because of the complexity of the structure, the lattice dynamics will have to remain at the relatively unsophisticated level of a rigid-ion model. At this point, it appears that only a complete inelastic neutron-diffraction experiment would yield enough information to carry the calculation any further. We have surmised possible

structures for 110.9 and 103 °K phase transitions, but we have left completely unanswered the whole question of the 76 °K transition and the mechanism that drives it. Thus, we are not yet in a position to understand completely the 12 °K magnetic transition and the elementary excitations that belong to that phase.

Nonetheless, the picture that has evolved during the course of these experiments and calculations is an extremely appealing one. The concept of a soft mode consistently ties together all of the experimental information that has been collected up to this point. It has allowed the interpretation of several previous results and has also allowed us to put quite stringent limits on the possible symmetries of the distorted phases. The lattice-dynamics calculation, on the other hand, gives a quantitative description of the major part of the experiments, namely, the spectroscopic data. In addition, it has allowed us to test and verify the concept of the soft mode.

ACKNOWLEDGMENTS

---

[1]W. Cochran, Phys. Rev. Letters 3, 412 (1959); Advan. Phys. 9, 387 (1960).

[2]P. W. Anderson, in Fizika Dielectrikov, edited by G. I. Skanavi (Academy of Sciences of the USSR, Moscow, 1960).

[3]R. A. Cowley, Phys. Rev. 134, A981 (1964); Phil. Mag. 11, 673 (1965).

[4]J. M. Worlock and P. A. Fleury, Phys. Rev. Letters 19, 1176 (1967).

[5]G. Shirane and Y. Yamada, Phys. Rev. 177, 858 (1969).

[6]R. H. Busey, H. H. Dearman, and R. B. Bevan, Jr., J. Phys. Chem. 66, 82 (1962).

[7]V. J. Minkiewicz, G. Shirane, B. C. Fraser, R. G. Wheeler, and P. B. Dorain, J. Phys. Chem. Solids 29, 881 (1968).

[8]M. E. Fischer, The Nature of Critical Points (University of Colorado Press, Boulder, Colo., 1966), Vol. VIIC.

[9]L. P. Kadanoff et al., Rev. Mod. Phys. 39, 395 (1967). (1967).

[10]L. D. Landau, Physik Z. Sowjetunion 11, 545 (1937); L. D. Landau and E. Lifshitz, Statistical Physics (Addison-Wesley, Cambridge, Mass., 1958).

[11]S. S. Mitra, in Solid State Physics (Academic, New York, 1962), Vol. 13, p. 2.

[12]M. Tinkham, Group Theory and Quantum Mechanics (McGraw-Hill, New York, 1964).

[13]V. Heine, Group Theory in Quantum Mechanics (Pergamon, New York, 1960).

[14]G. F. Koster, in *Solid State Physics* (Academic, New York, 1957), Vol. 5.

[15]J. L. Birmam, Phys. Rev. <u>127</u>, 1093 (1962); <u>131</u>, 1489 (1963); <u>125</u>, 1959 (1962).

[16]E. Burstein, F. A. Johnson, and R. Loudon, Phys. Rev. <u>139</u>, 1239 (1965).

[17]Faddeyev, *Tables of the Principle Representations of Fedorov Groups* (Pergamon, New York, 1964).

[18]S. C. Miller and W. F. Love, *Tables of the Irreducible Representations of Space and Co-Representations of Magnetic Space Groups* (Pruett Press, Boulder, Colo., 1967).

[19]B. Aminoff, Z. Krist. <u>94</u>, 246 (1936).

[20]D. Gribier, B. Farraux, and B. Jacrot, in *Inelastic Scattering of Neutrons in Solids and Liquids* (International Atomic Energy Agency Vienna, 1963), Vol. II, p. 225.

[21]G. Dolling, R. A. Cowley, and A. B. Woods, Can. J. Phys. <u>43</u>, 1397 (1964).

[22]M. Born and K. Huang, *Dynamical Theory of Crystal Lattices* (Oxford U. P., Oxford, England, 1954).

[23]L. Chen, R. Berenson, and J. L. Birman, Phys. Rev. <u>170</u>, 639 (1968).

[24]V. L. Ginzburg, Fiz. Tverd. Tela <u>2</u>, 2031 (1960)

[Soviet Phys. Solid State <u>2</u>, 1824 (1961)].

[25]W. Känzig, Solid State Phys. <u>4</u>, 1 (1957).

[26]See, for example, E. Fatuzzo and W. J. Merz, *Ferroelectricity* (Interscience, New York, 1967).

[27]G. P. O'Leary, Phys. Rev. Letters <u>23</u>, 782 (1969).

[28]K. R. Jeffrey and R. L. Armstrong, Phys. Rev. <u>174</u>, 359 (1968).

[29]H. Bayer, Z. Physik <u>130</u>, 227 (1951).

[30]R. Ikeda, D. Nakumura, and M. Kubo, J. Phys. Chem. <u>69</u>, 2101 (1965).

[31]L. A. Woodward and M. J. Ware, Spectrochim. Acta. <u>20</u>, 711 (1964).

[32]D. M. Adams and H. A. Gebbie, Spectrochim. Acta. <u>19</u>, 925 (1963).

[33]P. B. Dorain and R. G. Wheeler, J. Chem. Phys. <u>45</u>, 1172 (1966).

[34]T. Kushida, G. B. Benedek, and N. Bloembergen, Phys. Rev. <u>104</u>, 1364 (1956).

[35]I. I. Gol'dman and V. Krivchenkov, *Problems in Quantum Mechanics* (Addison-Wesley, Cambridge, Mass., 1961).

[36]G. N. Krynauw and C. W. F. T. Pistorius, Z. Physik. Chem. (Frankfurt) <u>43</u>, 113 (1964).

Magnetic Surface Modes: Classification, New Types, and Simple Method of Solution

M. Sparks[*]

Science Center, North American Rockwell Corporation, Thousand Oaks, California 91360

A physical interpretation of the eigenvalue equation is used to obtain the frequencies and spin configurations of ferromagnetic and antiferromagnetic surface modes and to provide a classification of these modes. A physical understanding of the features of surface modes also is provided. Since all spins precess at the same frequency in a normal mode, the frequency can be obtained from the equations of motion of one, or sometimes two or three, spins near the surface. One class of surface modes is the *changed-surface-parameter class*, in which the missing neighbors of a surface spin are compensated for by a changed parameter, such as an exchange constant, at the surface. Another is the *equivalent-layer class*, in which the crystal contains equivalent layers such that the net torque on each spin $\vec{S}$ on an equivalent layer exerted by all spins on the surface side of $\vec{S}$ is zero. Two new types of surface waves are studied. In the first, the spin precession changes phase as well as amplitude as a function of the distance from the surface. In the second, a surface layer of spins is antiparallel to the bulk spins.

1. INTRODUCTION

There have been a number of recent investigations of surface waves in magnetic systems.[1-7] In the present paper, a physical interpretation of the eigenvalue equation is used to obtain the normal-mode frequencies (eigenvalues) and the spin configurations (eigenvectors) of ferromagnetic and antiferromagnetic surface waves. An intuitive understanding of how the crystal can support the surface modes and of the physical features of the modes is afforded by the interpretation, which is used to classify surface modes and to study two

new types of surface modes. Simple physical explanations of existing results also are afforded by the method, which is applicable to all presently known exponentially decaying modes, both acoustical and optical.

In a normal mode, all spins precess at the same frequency, by definition. By requiring the frequency of a surface spin to be the same as that of a bulk spin and assuming a form of the solution for the bulk spins (exponential for surface modes), the normal-mode frequencies can be obtained. In particular, a spin on the surface will have fewer neighbors than a corresponding spin in the bulk,